Hindawi
Advances in Civil Engineering
Volume 2019, Article ID 9372505, 23 pages
https://doi.org/10.1155/2019/9372505

Research Article

Accuracy Assessment of Shake Table Device on Strong Earthquake Output

Wei Guo,[1,2] **Ping Shao**,[1,2] **Hai-yan Li**,[1,2] **Yan Long**,[1,2] **and Jian-feng Mao**[1,2]

[1]*School of Civil Engineering, Central South University, Changsha 410075, China*
[2]*National Engineering Laboratory for High Speed Railway Construction, Changsha 410075, China*

Correspondence should be addressed to Hai-yan Li; lindsay@csu.edu.cn

Received 7 July 2019; Revised 20 September 2019; Accepted 25 October 2019; Published 12 November 2019

Academic Editor: Ahmed Mebarki

In order to avoid unexpected damage of structural specimens in the test, at the beginning, a signal with small amplitude is adopted to input the shake table device to gain the transfer function and corresponding drive signal, and then a strong earthquake output can be reproduced by amplifying the drive signal proportionally. However, as there are obvious nonlinearities inherent in the shake table device and structural specimen under strong earthquakes, errors inevitably exist in the replayed and amplified earthquake output if the linear transfer function and the drive signal, which are obtained by the small amplitude input, are adopted, and the desired output signal cannot accurately be achieved. Considering this point, several typical structural experiments are introduced and analyzed in this paper to study the earthquake output accuracy of the large-scale shake table test, such as inertia and elastic specimens, large-span floor, isolated building, high-speed railway station, bridge piers, and collision of adjacent multispan bridges. The transfer function of the shake table device and structural specimen is described. The energy-time history (energy-TH) index can assess the accuracy of the shake table on the strong earthquake output in the aspect of specimens other than signals themselves. The double parameter performance table is established based on this energy-TH index. More attention should be paid to energy and amplitude for the reproduction of strong earthquakes, and the accuracy details of signal reproduction should not be too strict.

1. Introduction

Earthquake is a devastating and widespread natural disaster, which causes a serious threat to civil engineering and the safety of people's life and property [1]. In order to study seismic damage characteristics of structures, since the last century, quasistatic test, quasidynamic test, shake table test, and some other novel test technologies have been developed. Due to the quasistatic test cannot reflect the seismic records and quasidynamic test cannot reflect the rate-dependent effect, the shake table test is usually considered as the most effective way to reproduce seismic damage on structures [2, 3]. The first shake table was built in 1968, and since then, a considerable number of shake table and table array devices have been constructed worldwide. The most famous one is E-Defense in Japan's National Research Institute for Earth Science and Disaster Prevention which is also the largest one in the world. By the E-Defense table, the prototype model test of structure can be conducted to avoid size effect in the scaled model test. In the 1980s, a number of shake tables were set up in China, and in recent years, more devices were built. Until now, more than 50 shake tables have been built in China and most of them were produced by MTS and SERVOTEST. These shake tables are characterized by large-scale, array, and digital control.

In the case of extensive construction and development of the shake table, the rational use and maintenance of equipment is essential. However, since the vibration table involves more professional knowledge such as hydraulic, numerical control, mechanics, and civil engineering, there are still some key problems that have not been solved, such as accurate reproduction of strong earthquakes and nonlinear control of the vibration table system.

In 1973, Edwin and other scholars [4] successfully implemented the test of a random vibration power spectrum, which laid a solid foundation for the development of

the random vibration test. In 1988, Blondet and Esparza [5] studied the interaction between the shake table device and specimen, which is important to understand the behavior of the seismic simulator system near their operational limits. In Newell's work [6], a nonlinear model of the seismic simulator at the University of Notre Dame had been presented, and the validity of the numerical model is demonstrated experimentally. The dynamic modeling method of the single direction servo hydraulic shake table has also been adopted by Conte and Trombetti [7] in 2000. At the same time, Ogawa et al. [8] introduced the key technology of the large shake table of 1200 tons, which became the theoretical basis of the Japanese E-Defense shake table. In 2002, Trombetti and Conte [9] studied the dynamic characteristics of devices by comparing different shake table tests. In 2005, Chase et.al. [10] improved the parameter identification method of the shake table system, which replaced the white noise with the actual vibration, making the transfer function more effective. In 2007, Tagawa and Kajiwara [11] described the specification of the facility, features of the control system, and control performance of some tests. In 2008, Plummer [12] proposed a dynamic modeling method of the six-axis shake table, which laid the foundation for the shake table control and mechanism analysis.

The strategy, which combines the linear shake table assumption, feedback control, and multiple iterations to minimize the output error of earthquake reproduction by the shake table device [13], is widely used in industry. For the structural dynamic test, in order to avoid the unexpected damage to the structural specimen, a white noise signal with small amplitude is firstly adopted to input the shake table to gain the transfer function of the system. The transfer function identified by the white noise may not fit the shake table carrying out real seismic records. Hence, the multiple iteration process is adopted. A seismic acceleration with small amplitude is replayed for several iterations to gain the appropriate drive signal. The drive signal can improve the signal reproduction accuracy of the shake table. Then, the strong earthquake output is reproduced by proportionally amplifying the obtained small drive signal.

However, this strategy is based on the premise that the whole system composed of the shake table and specimens is linear. When strong earthquake acceleration is outputted by the shake table, specimens may be damaged. Both shake table and specimen are nonlinear. The accurate output of strong earthquake is not easy to achieve. Therefore, it is necessary to clarify whether the linear model identified by the small-scale excitation input is applicable to large earthquakes. In this paper, the corresponding research work is carried out in detail. The energy-time history (energy-TH) index and the double parameter performance table of strong earthquake output of the shake table device are proposed to assess the accuracy of the shake table device on strong earthquake output. The energy-TH can be used to assess the output accuracy of the shake table in the aspect of test specimens. The numerical model of the high-speed railway station was built to verify the energy-TH index can better reflect the influence of output precision of the shake table on structural response than other indices. Those results can provide a reference for rationally performing the shake table test and evaluating the device performance.

2. Influence Factors on Accuracy of Strong Earthquake Output

The accuracy of strong earthquake output of the shake table depends on the device performance and the specimen. The performance of the shake table device is the key factor, and its inherent nonlinear performance significantly affects the linear correlation of earthquake output under different magnitudes. The weight and stiffness of specimens, which generally exert the feedback force to the shake table, also have significant effect on the strong earthquake output. There exists an obvious specimen-shake table interaction. Meanwhile, the specimens may crack and damage subjected to strong earthquake output, and the nonlinear characteristic of specimens exists in the test. The control of the shake table device should be adjusted accordingly, but in fact, the control is still designed in the framework of linear assumption, which cannot take the nonlinearity into account. The following section discusses the influence of the device and specimen on the strong earthquake output.

2.1. Device Components and Nonlinearity. The seismic simulation shake table array in National Engineering Laboratory for Construction Technology of High-Speed Railway at Central South University (CSU) in China consists of four three-dimensional six-degree-of-freedom (DOF) shake tables, analog and digital control system, and hydraulic power system. One of shake tables at CSU in Figure 1(a) consists of a table, mechanical support, and hydraulic actuators. The technical specifications of the shake table array are shown in Table 1. The performance parameters of each shake table of the array are the same.

The table and the mechanical support system usually have enough rigidity in order to prevent the vibration resonance and ensure the stability and safety during the test. As a result, when designing the feedback control of the shake table, the table and mechanical support can be taken as a rigid body. The actuator is the exciting device of the shake table, which converts hydraulic pressure into mechanical energy. In the control element of the actuator, servo valve, electrical signals are amplified to spool signals firstly and then are converted to oil signals. The sensor feeds back displacement signals of actuators to the control system. Several complex factors affect the performance of the hydraulic actuator in the process, such as time delay of servo valve and oil leakage. The hydraulic power system in Figure 1(b) includes oil tank and pumps. It provides power for the hydraulic system. Electric energy is converted into mechanical energy and then into hydraulic energy. It is the power core of the shake table system. Due to the complex factors and the hydraulic oil characteristics, the shake table system is inherently nonlinear. The analog and digital control system is the part that receives analog and digital signals and decides to send signals through the control algorithm, which is equivalent to the brain of the shake table

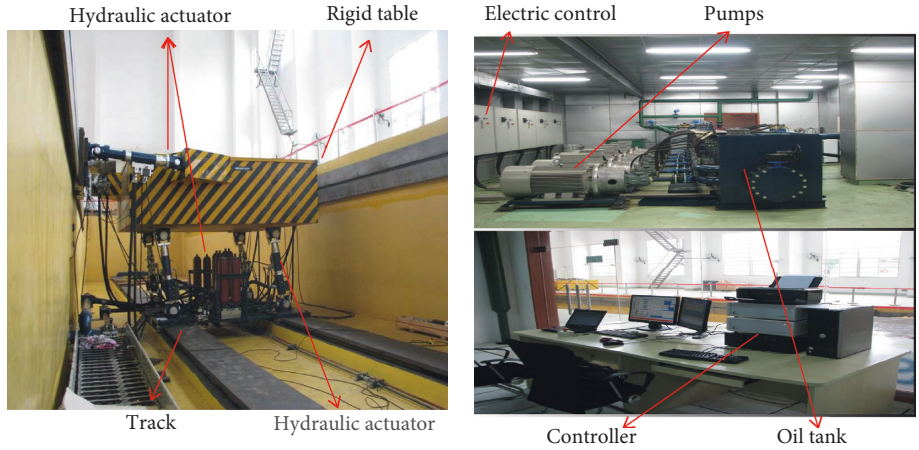

Figure 1: Shake table device's important components. (a) Shake table and hydraulic actuator; (b) pump station, oil source, and control system.

Table 1: The technical specifications of the shake table array at CSU.

Items	Dynamic specifications
Number of shake tables	4
Degrees of freedom	6 (each table)
Size	4 m × 4 m
Mass	13 ton
Maximum specimen load	30 ton (each table)
Maximum displacement and acceleration (full load)	X 250 mm, ±0.8 g Y 250 mm, ±0.8 g Z 160 mm, ±1.6 g
Maximum velocity	1000 mm/s
Frequency range	0.1–50 Hz

system. The effectiveness and stability of the algorithm are very important.

The control system of the shake table includes iterative control system (ICS) and PID control. ICS is used to improve the control accuracy of the PID control. As shown in Figure 2, the shake table is a six-DOF device driven by eight actuators. The PID control is used as servo control for each DOF of the shake table. The geometric transformation helps signals to transform between six DOFs and axial direction of eight actuators.

ICS is a control method that identifies the shake table model and iteratively modifies the drive signal offline to make the output of the shake table consistent with the desired signal. Because the PID control with fixed parameters used as servo control has insufficient control accuracy for tests of different specimens, ICS is selected to improve the control accuracy. The shake table test procedure using ICS is shown in Figure 3. The process is mainly divided into two parts: system identification and drive signal correction [14]. The shake table model is identified by inputting white noise to the shake table. By inversing the shake table model to minimize the error between desired signal and shake table output iteratively until it is smaller than preset tolerance ε, the drive signal for the formal test is obtained. In order to prevent the specimen from entering the plasticity or damage in advance during the iteration process, such as iteration for strong earthquake reproduction, the input signal should be reduced by a factor of k in the iteration. When the drive signal is obtained, it will be linearly amplified by k times for the formal test.

This control strategy for the shake table system is used widely all over the world. It is designed on the basis of the assumption that the shake table and specimen are linear. However, there exist various types of nonlinearity in the shake table device. As a result, the linear control theory characterized by transfer function is not feasible. The accuracy of the earthquake output of the shake table device is inevitably affected and should be assessed.

2.2. Influence of Specimen on Accuracy. As mentioned above, because of the reaction force of the specimen on the shake table, the shake table output will be affected. The strength of the influence mainly depends on the mass, stiffness, and nonlinear characteristics of the specimen. Large-mass specimens will have a greater impact on the shake table intuitively, but at present, for large-mass rigid specimens, it is easier to achieve accurate seismic output through shake table equipment control. However, civil engineering specimens often have certain mass and stiffness and have natural frequencies falling in 0.1–50 Hz. This overlaps with the working frequency of the shake table system and the natural frequency range of oil column, which may lead to a certain degree of resonance and affect the accuracy of seismic output. MTS, Servotest, and other shake table manufacturers have adopted a variety of strategies, such as three-parameter control and internal and external control loops, to optimize the control effect of the resonance frequency band. For the above method of determining the transfer function and drive signal for small-scale excitation and realizing strong earthquake by linear amplification output, the accuracy is not easily guaranteed after the specimen enters the stage of

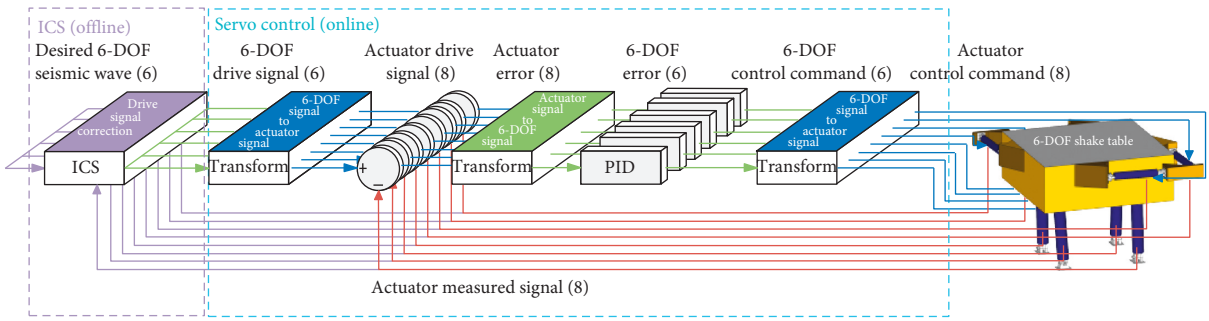

Figure 2: The control system of the shake table at Central South University.

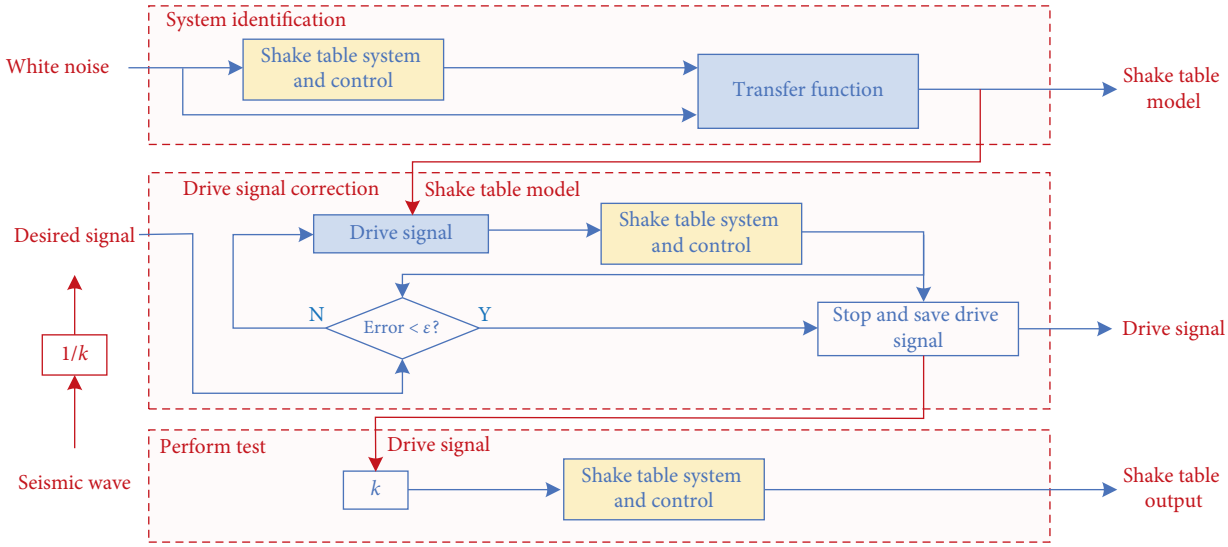

Figure 3: Flow diagram of ICS.

elastic-plastic damage, and the varying reaction force will affect the accuracy of strong earthquake reproduction.

2.3. Assessment Index of Accuracy. The accuracy of strong earthquake output of the shake table can be assessed by three indices: root-mean-square (RMS) error r [15], time-domain error e [16], and correlation coefficient c. If the desired time-history signal is $\mathrm{d}(t)$ and the actual output signal is $p(t)$, three indices are expressed as follows:

$$r = \left| \frac{\mathrm{rms}(\mathrm{d}(t)) - \mathrm{rms}(p(t))}{\mathrm{rms}(d(t))} \right|, \tag{1a}$$

$$e = \mathrm{mean} \frac{|\mathrm{d}(t) - p(t)|}{\max|d(t)|}, \tag{1b}$$

$$c = \frac{\mathrm{Cov}(\mathrm{d}(t), p(t))}{\sqrt{D(d(t))}\sqrt{D(p(t))}}, \tag{1c}$$

where rms means RMS, max is the maximum value, Cov denotes the covariance, and D is the variance. Time-domain error e is the average of error percentage at each time point of two signals, which has a relative value compared with the maximum peak value. The closer to zero the error is, the smaller the deviation between the two signals is. It is well recognized that when the error is between 0 and 0.35 [17], the difference between the two signals can be considered to be very small. This index describes the comprehensive error level caused by amplitude and time delay. In the test, the large amplitude at some time point of the signal may cause damage for some components. Time-domain error can in some extent reflect the influence of signal reproduction error on this kind of response of the specimen. However, if the response is insensitive to the time points with large error, the response of the specimen will not be influenced. Therefore, the time-domain error has limitations for the evaluation of the output signal. The effective evaluation index should consider the influence of the signal reproduction error on the specimen.

Correlation coefficient c is a statistical method to describe the similarity between two signals. The closer to 1 the correlation coefficient is, the more similar the two signals are. Statistically speaking, it is generally believed that two signals are highly correlated when the correlation coefficient falls between 0.8 and 1 [18]. The index includes amplitude and phase errors and is more stringent. When the similarity of the output signal and desired signal is high, it can be considered that the shake table is well controlled. But in the special case of two signals with low similarity and same energy, the responses of the specimen under two signal

excitations may also be similar. The response and damage of the specimen are not considered in the correlation coefficient.

RMS error can describe the difference in energy between two signals. It reflects the error of energy transmitted from signals to the specimen. The cumulative energy transferred from the shake table output signal to the specimen may cause structural failure. This index includes the influence of output errors on the cumulative damage of the specimen. It is one of the main indices to judge the control accuracy of the shake table. In industry, RMS error is used to judge whether the offline iteration converges to tolerance, and it is common that 0~0.2 is chosen as the convergence criterion. But to some extent, this index cannot describe the change in signal amplitude, while the amplitude of the seismic signal is one of the important indices concerned in the structural dynamic test. The two signals with similar energy differ in the peak value, which may lead to different damage results in the test.

In the research of this paper, the specimen is the concern of test, so the selected index should consider the influence on structural response and damage except the reproduction accuracy of the signal.

Frequency-domain analysis is also one of the important means in the evaluation of shake table signal reproduction accuracy. In industry, frequency-domain signals corresponding to the desired signal and actual output signal are used to judge the offline iterative convergence. In this paper, an equation for calculating the frequency-domain error is as follows:

$$e_f = \max\left(\frac{\left|D_f - P_f\right|}{\max\left|D_f\right|}\right), \tag{2}$$

where P_f is the FFT of the actual output signal $p(t)$ and D_f is the FFT of the desired time-history signal $d(t)$.

The shake table test is an important means to study seismic damage of structures. The influence of the shake table signal reproducing error on structural response is an important issue. The most widely used damage assessment model, Park–Ang [19], has identified that the maximum displacement and hysteretic energy dissipation of the structure are the most important. Therefore, the index should reflect the influence on structural response rather than the simple signal contrast. The structural response may be related to both the amplitude and energy deviations of the output signal, but none of the above indicators is related to these at the same time.

Equation (1a) for seismic energy and equation (1b) for the displacement should be combined, by which a new index is put forward, which can be referred to as the index of energy and displacement:

$$b = \alpha r + (1-\alpha)\max(\text{abs}|e|) = \alpha r + \beta \max(\text{abs}|e|), \tag{3}$$

where α and β are, respectively, the combination coefficients, referring to the relative importance of energy and displacement, which are determined according to the actual test. In this paper, to statistically evaluate the difference of four indexes for different specimens on the same standard, the amplitude and energy are considered equally important to the dynamic response of specimens. As a result, α and β are both set as 0.5. The new index of energy-TH index b synthetically evaluates the difference between two signals in terms of signal energy, amplitude, and phase. It describes the magnitude and energy difference of two signals transmitted to the specimen. Here, a double parameter performance assessment table is given as shown in Table 2. By calculating parameters b and c of different types of tests, the performance of the shake table can be assessed to directly provide a reference for the future shake table test.

3. Typical Shake Table Tests of Strong Earthquake Output

In this section, several typical shake table tests are introduced to analyze the device performance, which can be a reference for the same type of tests. Mass and natural frequencies of specimens usually have different effects on the output of the system composed of the shake table and specimens. In order to fully analyze shake table performance, a certain range of mass and natural frequencies is covered by specimens chosen. Two types of specimens are selected: building and bridge. Both these types include cases that are heavier than or lighter than 15 ton (50% of shake table capacity), and the distribution of natural frequencies of specimens is more dispersed. The asymmetric specimen on the shake table belongs to eccentric load. The shake table needs additional control performance to balance the eccentric force, which may affect the output of the shake table. Therefore, an asymmetric building, the isolated building (IB), is selected for analysis. Specimens include the inertial and elastic specimens, large-span floor (LS), isolated building (IB), high-speed railway station (HS), bridge piers (HP), and collision of adjacent multispan bridges (CB). Information of mass and the resonant frequency of each test specimen is shown in Table 3. According to Table 3, resonant frequencies of all these specimens fall in the working frequency range 0.1–50 Hz of the shake table.

Structural dynamic analysis includes acceleration excitation and displacement excitation. The main frequency range of seismic signal and the direction of loading may affect the seismic signal reproduction accuracy of the shake table. Therefore, in order to fully analyze shake table performance, test signals including acceleration excitation and displacement excitation are selected. Seismic signals with different main frequency ranges are considered. For the same shake table test, signals with different peak values and vibration directions are chosen.

For convenience, different combinations of seismic signals and structural types are numbered and shown in Table 4. In total, 32 test cases are included in this section.

3.1. Inertia and Elastic Specimens. The inertia and elastic specimens that possess linear dynamic characteristics are usually designed and tested in the shake table qualification acceptance. The inertia and elastic specimens for the shake table acceptance test at Central South University in China are introduced here. The inertia specimen is a sand box with

Table 2: Shake table performance assessment strategy based on the double parameter indices.

Performance index 1		Correlation coefficient c			
Performance index 2		Level 1 ($C1 < c < 1$)	Level 2 ($C2 < c \le C1$)	Level 3 ($C3 < c \le C2$)	Level 4 ($c \ge C3$)
Energy-TH index b	Level 1 ($b \le B1$)	Case $x1\ldots$	Case $x5\ldots$	Case $x9\ldots$	Case $x13\ldots$
	Level 2 ($B1 < b \le B2$)	Case $x2\ldots$	Case $x6\ldots$	Case $x10\ldots$	Case $x14\ldots$
	Level 3 ($B2 < b \le B3$)	Case $x3\ldots$	Case $x7\ldots$	Case $x11\ldots$	Case $x15\ldots$
	Level 4 ($B3 < b$)	Case $x4\ldots$	Case $x8\ldots$	Case $x12\ldots$	Case $x16\ldots$

$B1$~$B3$ are the reference limit values of index b and $C1$~$C3$ are the reference limit values of index c, which are determined based on the shake table device.

Table 3: Mass and resonant frequency of five specimens.

Test	Specimen mass (ton)	Resonant frequency (Hz)		
		First order	Second order	Third order
IB	23	2.51	2.56	5.7
LS	21.48	25.5	27.5	34.5
HS	13.98	10.6	15.4	27.0
HP	11	4.4	9.6	—
CB	21.34 (on each table)	1.98	—	—

Table 4: Working cases with different earthquakes and structural types.

Serial number	Test cases
LS-1	El-centro seismic records, 0.96 g
LS-2	El-centro seismic record, 1.54 g
LS-3	Taft seismic record, 1.18 g
LS-4	Taft seismic record, 1.94 g
LS-5	Wenchuan seismic record, 0.88 g
LS-6	Wenchuan seismic record, 1.42 g
LS-7	Wenchuan seismic record, 1.77 g
IB-1	Chichi-Y seismic record, 0.07 g
IB-2	El-centro-Y seismic record, 0.07 g
IB-3	PEL-Y seismic record, 0.07 g
IB-4	El-centro-X seismic record, 0.10 g
IB-5	El-centro-X seismic record, 0.07 g
IB-6	Pasadena seismic record, 0.42 g
HS-1	El-centro-Y seismic record, 0.16 g
HS-2	El-centro-Y seismic record, 0.74 g
HS-3	El-centro-Y seismic record, 0.44 g
HP-1	North bridge seismic record, 0.20 g-X
HP-2	North bridge seismic record, 0.20 g-Y
HP-3	North bridge seismic record, 0.11 g-X
HP-4	North bridge seismic record, 0.44 g-Y
HP-5	North bridge seismic record, 0.24 g-X
HP-6	North bridge seismic record, 0.24 g-Y
HP-7	North bridge seismic record, 0.28 g-X
HP-8	North bridge seismic record, 0.28 g-Y
CB-1	Artificial seismic record C5, 38 mm
CB-2	Artificial seismic record C5, 85 mm
CB-3	Artificial seismic record C5, 64 mm
CB-4	Artificial seismic record C, 14 mm
CB-5	Artificial seismic record S2, 9.3 mm
CB-6	Artificial seismic record S6, 7.4 mm
CB-7	Artificial seismic record Un C, 38 mm
HS-4	El-centro-X seismic record, 0.13 g

a mass of 18.5 tons, while the elastic specimen can be considered as a single degree of freedom with a natural frequency of about 4 Hz. The model and test cases are shown in Figure 4.

Seismic simulation is realized by the shake table. The working oil temperature of the equipment is 40 C, which is close to the ideal temperature. The transfer functions of the shake table under different loads are identified by inputting white noise. As shown in Figure 5, the linearity of the transfer function under inertial load is better, while there are obvious frequency resonance points and range segments under elastic load.

Kobe earthquake with the peak ground acceleration (PGA) of 0.8 g was chosen as the desired signal. The shake table's output signal without iteration is shown in Figure 6(a), and it is obvious that the error between acceleration output and the desired signal is large, especially for PGA. If the phase difference between the desired signal and actual output signal of seismic acceleration is neglected, the RMS error is 30%. Through the ICS of the shake table, the drive signal was adjusted to reduce the error on the premise that the transfer function remained unchanged. After four iterations, the RMS error is reduced to 5%. At this moment, the shake table accurately outputs the desired signals. The results in Figure 6 show that the shake table under ICS can achieve better accuracy.

3.2. Large-Span Floor Specimen. Seismic performance of the large-span floor in the high-speed railway station is tested by the shake table. The similarity coefficient of the model is 1 : 20, and numerical and physical models are shown in Figure 7. By the white noise input, the transfer function of the shake table together with the specimen is calculated and shown in Figure 8. The curve of the transfer function shows good correlation between desired and output signals except the frequency resonance point. In the shake table's output with small magnitude, the first and 4 iterations are both shown in Figure 9. The error of the earthquake output can be well diminished by iteration. Figures 10(a)–10(c) give outputs of strong earthquakes, which indicate good accuracy of desired signal's reproduction. In Figure 10(d), four indices above are adopted to calculate errors of output signals compared with desired signals. It shows that the shake table is well controlled as a linear system and behaves with high accuracy in most test cases. The energy-TH index of most cases can be controlled within 10%, and the similarity between the desired and the output signals reaches 90%. The correlation coefficient of LS-5 is the smallest, while the correlation coefficient of LS-2 is the largest in all the cases. It means the similarity of desired and output signals in LS-2 is better than that in other cases. However, the RMS error in LS-2 is larger than that in LS-3. Hence, there is more energy

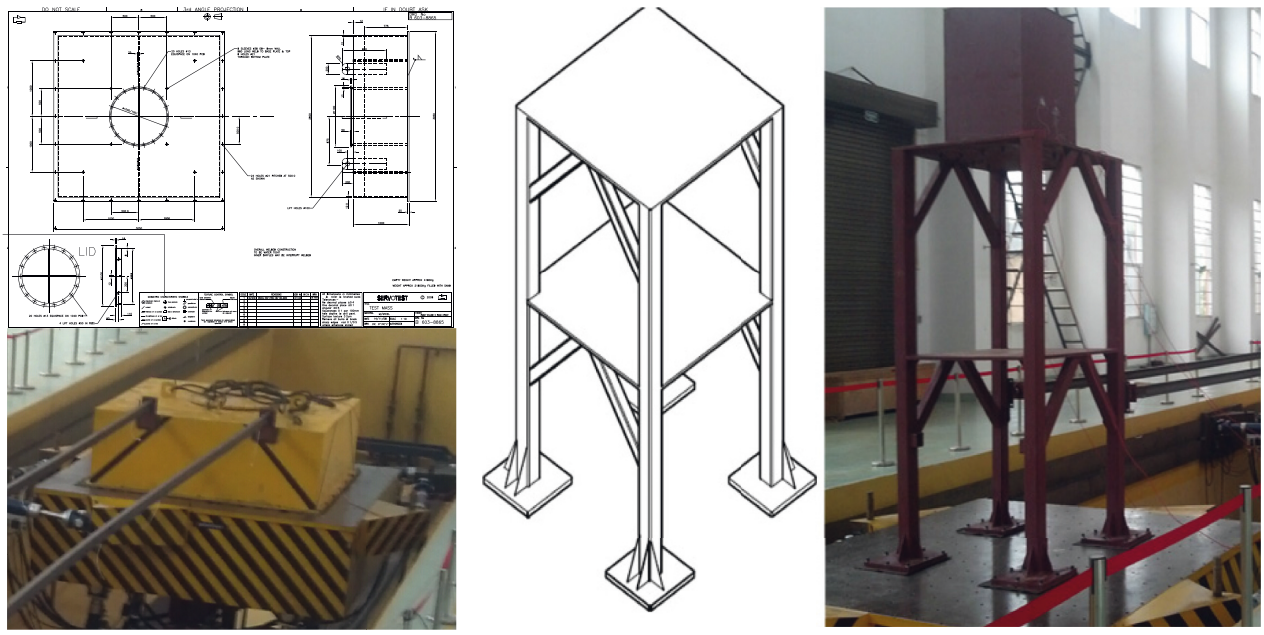

(a) (b)

Figure 4: Shake table test with (a) inertia and (b) elastic specimens.

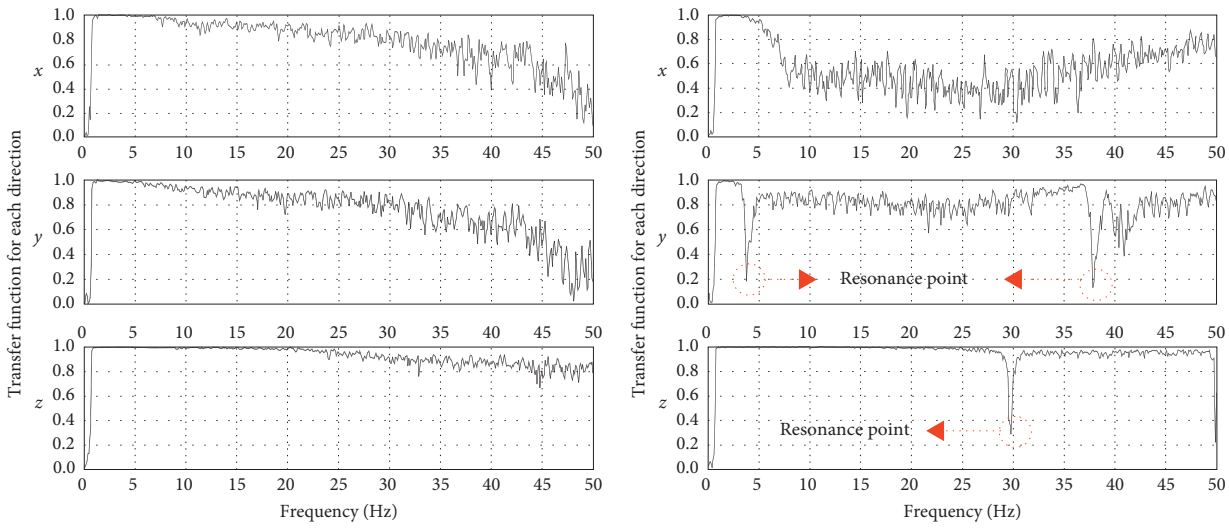

(a) (b)

Figure 5: Transfer functions of the shake table device with (a) inertia and (b) elastic specimens.

difference in LS-2. The RMS value of the desired signal in LS-3 is the smallest which means, in other cases, there is a greater energy difference between desired and output signals. But the time-domain error of case LS-3 is slightly larger than that of other cases which means the average amplitude difference does exist between desired and output signals. As a result, in the case of LS-3, the error of desired and output signals has greater effect on the structural damage caused by excessive signal amplitude, but less effect on the structural damage caused by energy accumulation. Different indices may draw opposite conclusions. Considering amplitude and energy of the signal, the energy-TH index of LS-3 is the smallest, and signal reproduction in LS-3 is good from the prospective of structural response.

Figure 11 gives the frequency-domain reproduction results of different cases and the maximum frequency-domain errors of all the cases. Compared with other four indices, it shows different trends. The maximum frequency error of LS-4 is the smallest, while its time-domain error is the largest. And another three indices are all larger than other cases in all the test cases of test HS. The maximum frequency-domain error of LS-3 is as high as 0.59, and the frequency-domain accuracy is low.

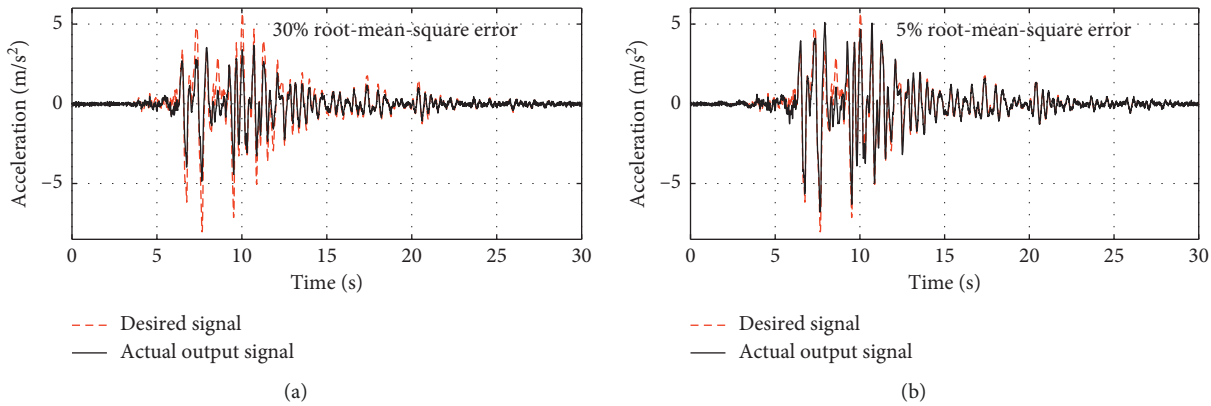

Figure 6: Comparison of the output signal and desired signal of Kobe earthquake with 0.8 g PGA. (a) Output without iteration; (b) output with 4 iterations.

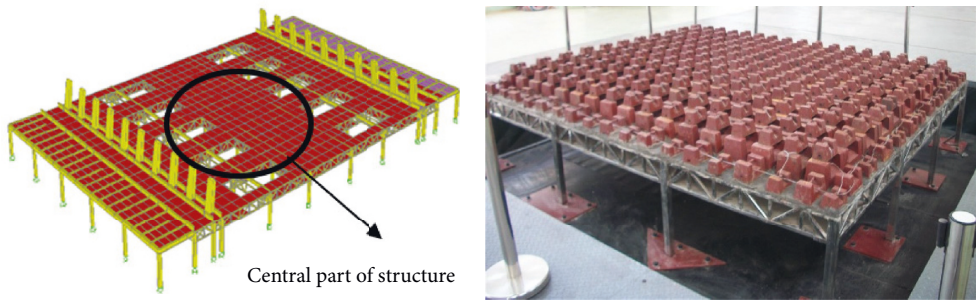

Figure 7: Shake table test with large-span floor specimen. (a) Numerical model; (b) test specimen.

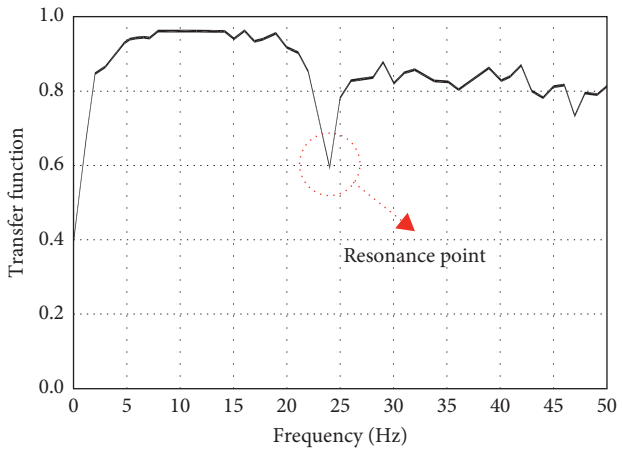

Figure 8: Transfer function of the shake table and specimen.

3.3. Isolated Building. The isolated building is built upon a metro in Shenyang city, and the isolation is set between the metro station and upper tall buildings, which are shown in Figure 12. The similarity ratio of the shake table mode is 1 : 20. The output signals of the shake table and corresponding error of different earthquake outputs are shown in Figure 13. The RMS error of the strong earthquake output is controlled within 20%, and linear correlation coefficient is about 40%–90%. Results show that the correlation coefficient of IB-1 is the smallest. However, the correlation coefficient of IB-5 is the closest to 1 in all the cases which means the similarity of desired and output signals in IB-5 is better than that in other cases. Otherwise, as for the energy, the RMS error in IB-5 is larger than that in IB-4. The RMS error in IB-4 is the smallest, and there is nearly no significant energy difference between desired and output signals. However, the time-domain error in the IB-4 case is slightly larger than that in other cases. Considering time-domain error and energy error of the seismic signal, the energy-TH index of IB-4 is the smallest. Compared with other cases, the overall performance of signal energy and amplitude reproduction of this test case is the best. In the case of IB-2, the desired signal and the output signal are similar, while the RMS error and the time-domain error are larger. The correlation coefficient, RMS error, or time-domain error alone cannot effectively evaluate the influence of the shake table output on the test specimen.

Figure 14 gives the frequency-domain reproduction results of three test cases corresponding to Figure 13 and the maximum frequency-domain errors of all the test cases. The maximum frequency-domain errors of all the test cases show the same trend with correlation coefficient, RMS error, and energy-TH index. But it has a different trend with time-domain error. The time-domain error of IB-2 is larger than those of cases 1, 3, and 4, while the other indices are smaller. The time-domain error should not be used to estimate test error independently.

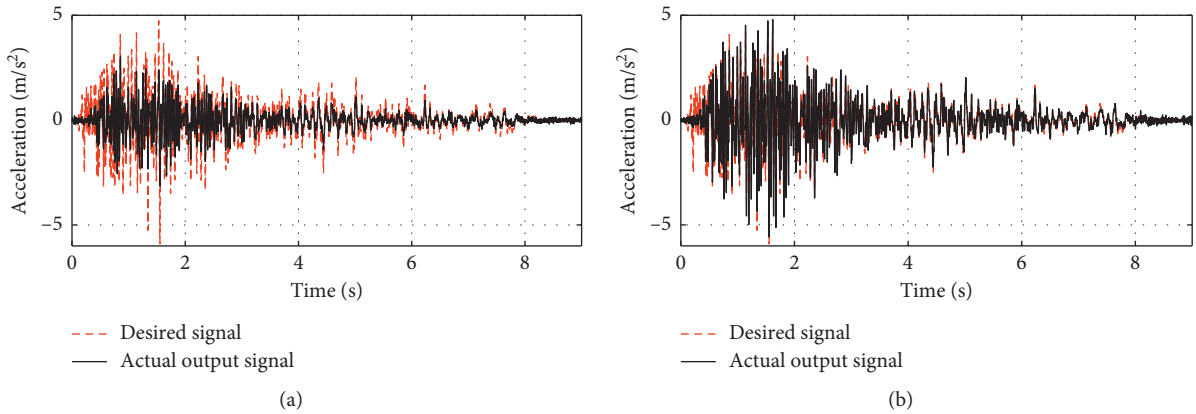

FIGURE 9: Comparison of the output signal and desired signal of the Taft earthquake with 0.50 g PGA. (a) Output without iteration; (b) output with 4 iterations.

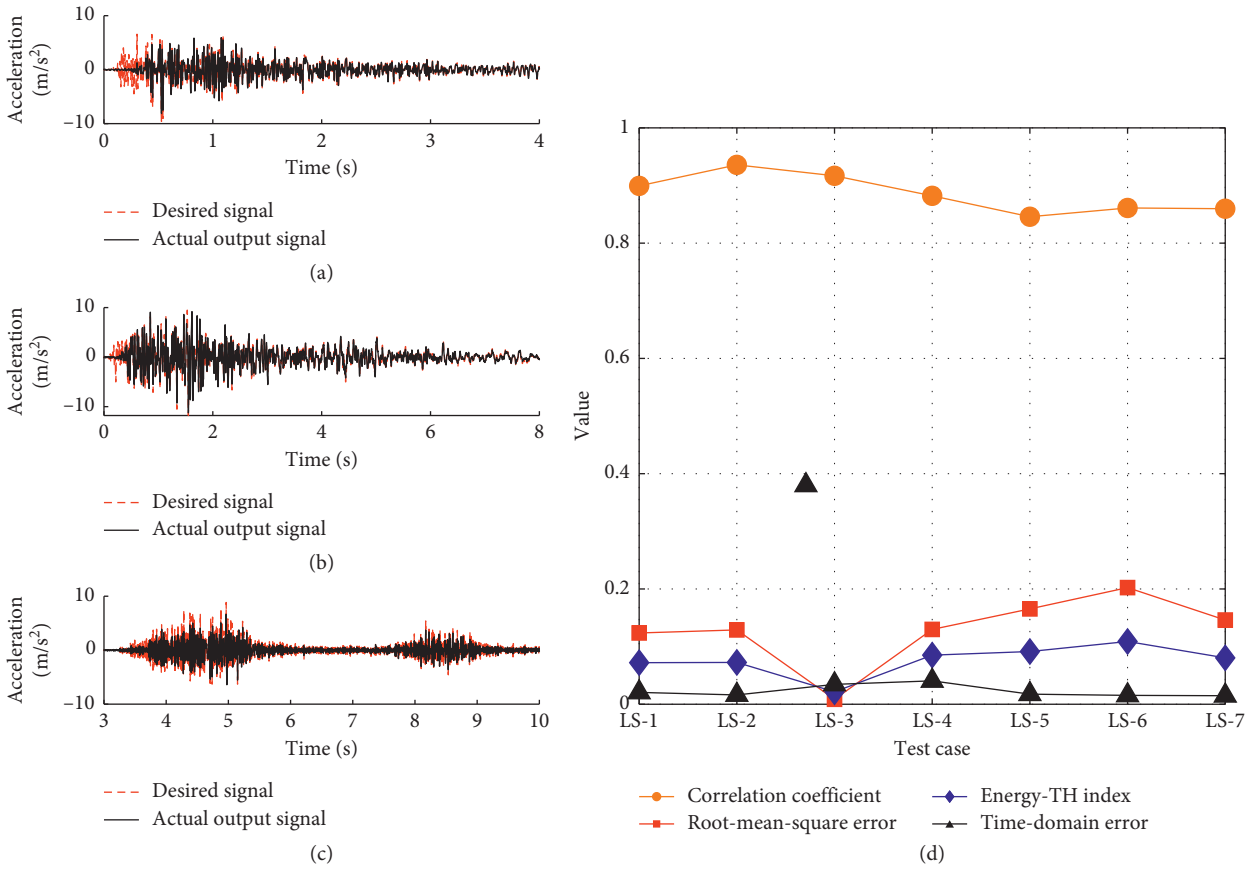

FIGURE 10: Shake table's output and corresponding error of different test cases with large-span roof. (a) Case LS-1; (b) case LS-3; (c) case LS-5; (d) output error of test cases.

3.4. High-Speed Railway Station. The central part of the Tianjin West railway station, which is a typical building-bridge integrated structure, was tested by using the shake table device. The similarity ratio of the model is set to be 1 : 20. Numerical and test specimens are shown in Figure 15, and the total weight of the specimen is about 20 tons. The outputs of earthquake acceleration and corresponding error of different earthquake outputs are shown in Figure 16. The correlation coefficient of HS-3 is the smallest among the four test cases, while the correlation coefficient of HS-1 is the largest among all the test cases. Therefore, the similarity of desired and output signals of HS-1 is better than those of other test cases. However, from the energy point of view, the error of HS-1 is larger than that of HS-2. The RMS value of HS-2 is the smallest, but there is still difference in the energy between the desired and the output signals. However, the

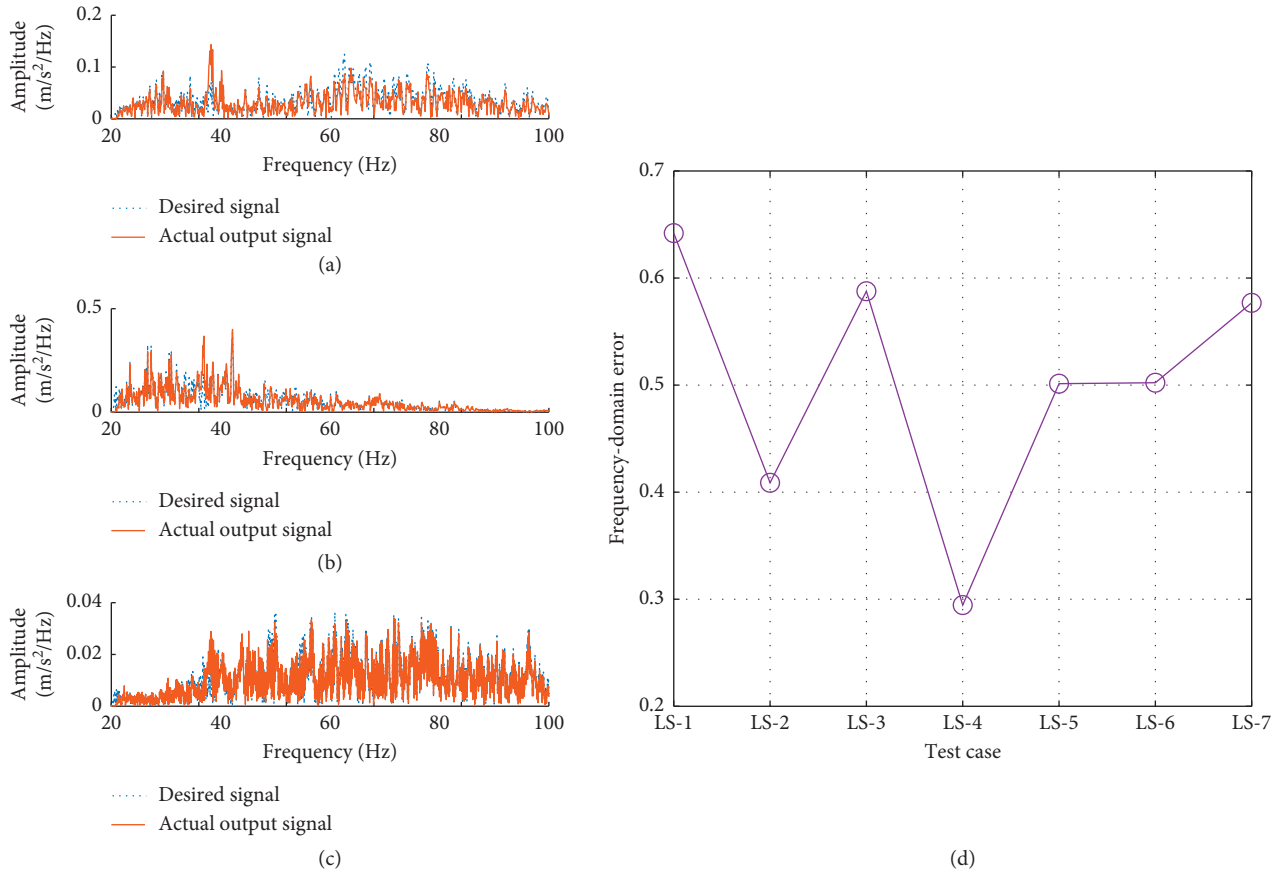

Figure 11: Desired signal and actual output signal frequency-domain comparison and error. (a) Case LS-1; (b) case LS-3; (c) case LS-5; (d) frequency-domain error of test cases.

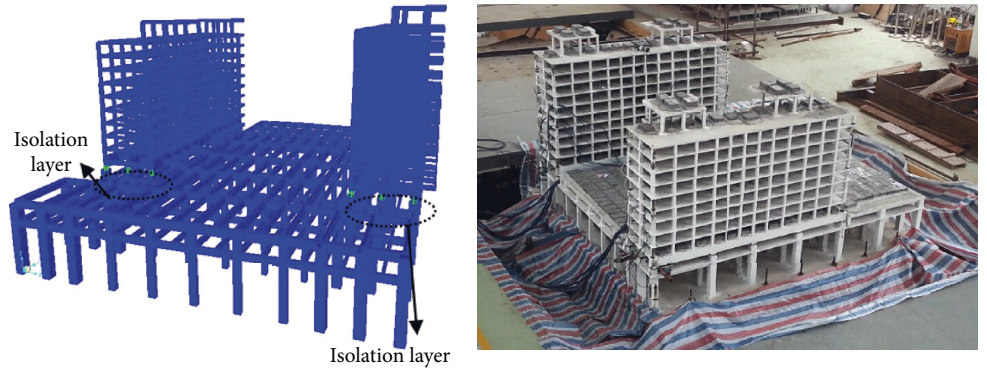

Figure 12: Shake table test with isolated building. (a) Numerical model; (b) test specimen.

time-domain error of HS-2 is larger than those of other cases, and the average amplitude of desired and output signals differs greatly. Considering the time-domain error and energy error, the energy-TH index of HS-2 is the smallest. Compared with other test cases, the overall performance of signal energy and amplitude reproduction of this test case is the best. The RMS error is still 40% after iterations. The linear control and iteration strategy cannot ensure the shake table device to reproduce the desired signal of different earthquake accelerations for all kinds of specimens.

Figure 17 gives the frequency-domain reproduction results of three test cases and the maximum frequency-domain error of all the test cases. The trend of the frequency-domain error is like it of the time-domain error and the correlation coefficient, and error of HS-2

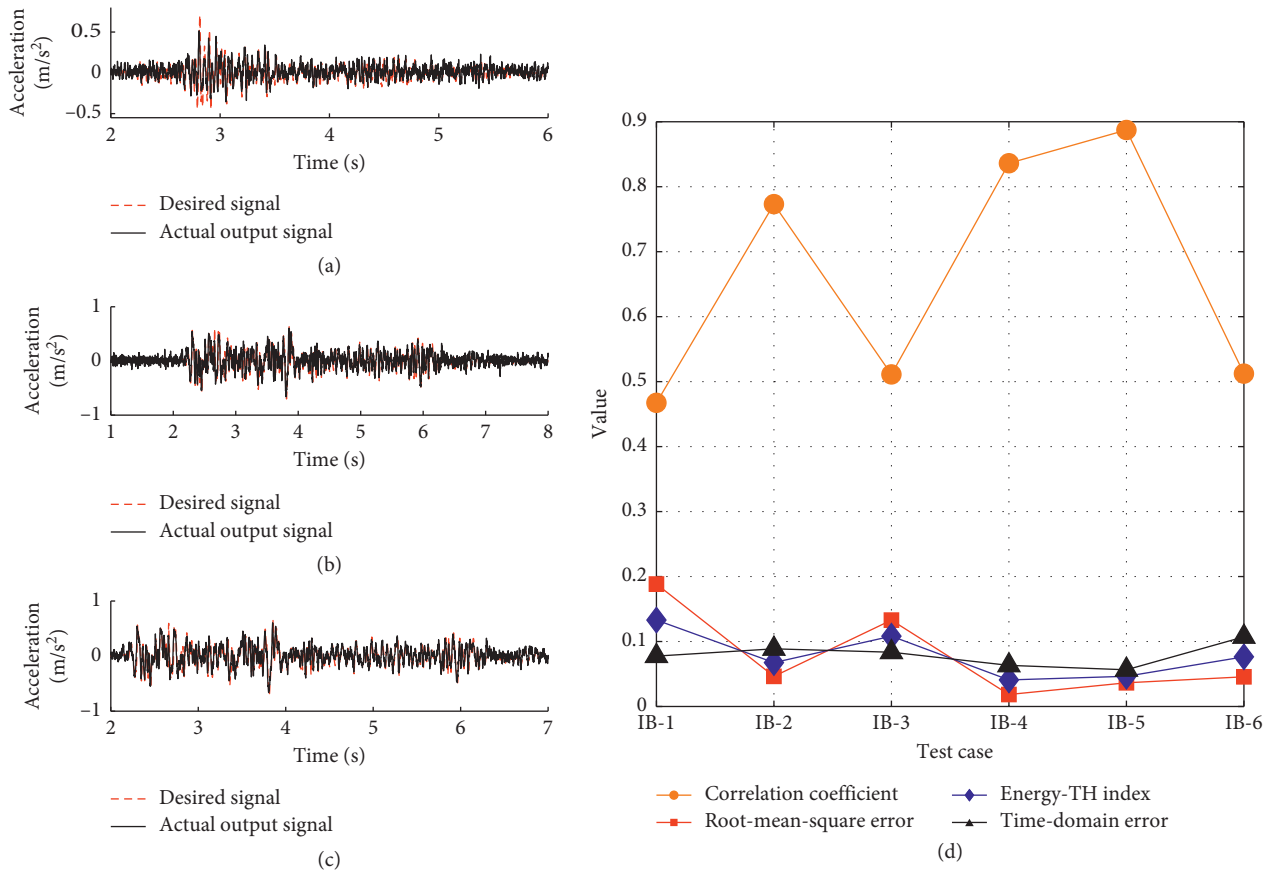

FIGURE 13: Shake table's output and corresponding error of different test cases with isolated building. (a) Case IB-1; (b) case IB-2; (c) case IB-3; (d) output errors of test cases.

and HS-3 is larger than that of others. However, RMS error shows a contrary trend. When errors of amplitude and energy are opposite, the energy-TH index is necessary.

3.5. High-Speed Railway Bridge Piers. The performances of a series of high-speed railway bridge piers have been tested by using the shake table device. As the high-speed railway bridge piers are usually built to be very stiff with high natural frequency [20], the coupling effect of piers with the shake table is not obvious because of no frequency resonance. Numerical and physical test specimens are shown in Figure 18. The similarity ratio for piers is 1 : 10. The outputs of earthquake acceleration and corresponding error of different test cases are shown in Figure 19. By carrying out different test cases, it shows that the RMS error of the strong earthquake output of the shake table device can be controlled within 5%, and the correlation coefficients is about 0.95, which represents a considerable high output accuracy of the shake table device in the cases of no resonance. The correlation coefficients are close to 1 in all eight cases, which indicates that the desired signals and the output signals are very similar. The RMS errors and the time-domain errors of the eight cases are close to 0. It means that the energy and the average amplitude of the desired and the output signals are almost identical. The energy-TH index of each case is close to 0, which indicates that the signal reproduction is accurate, and the results are the same as those of other indicators. For tests with high precision of signal reproduction, four indices show that test errors are very small, and there is no obvious difference between them.

Figure 20 gives the frequency-domain reproduction results of three test cases and the maximum frequency-domain error of all the test cases. The frequency-domain error shows the opposite trend with the RMS error. The maximum frequency-domain error of HP-4 is the smallest while the RMS error is the largest in all the test cases of test HP. For other indices, signal reproduction in the HP test case is accurate. But the frequency-domain error of HP-4 is large. The relative error at each frequency of HS-4 is shown in Figure 21(a), and the maximum error is at 6.9 Hz. After being processed by 6~8 Hz bandpass filter separately, the time history of the desired signal and actual output signal are compared in Figure 21(b). The maximum amplitude error of the filtered time-history signal is 5% relative to the peak acceleration of the unprocessed desired signal. As a result, the frequency error at 6.9 Hz has inconspicuous effects on the reproduction of desired time history, and the reproduction accuracy of HP-4 is well. Hence, the frequency-domain error may exaggerate that the reproduction error should not be used to estimate test error independently.

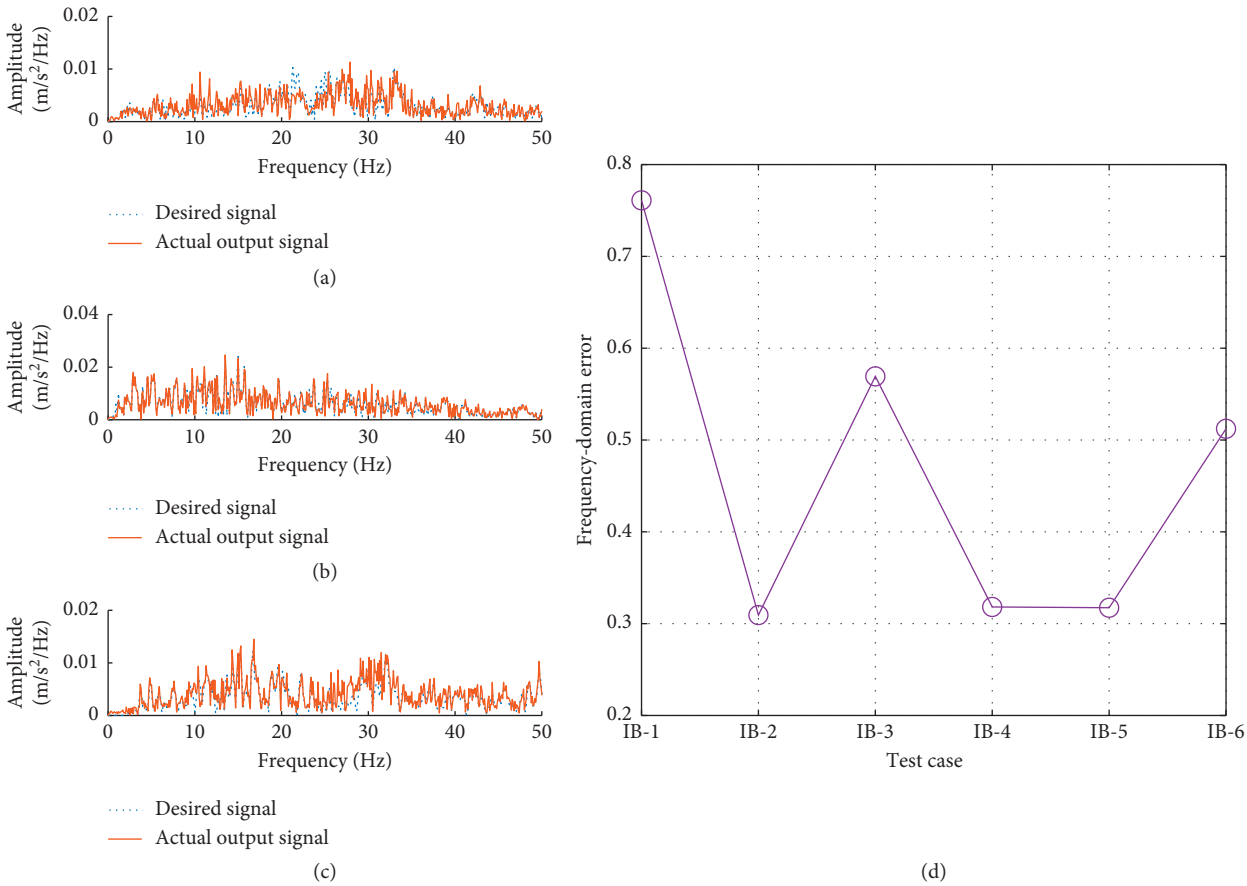

Figure 14: Desired signal and actual output signal frequency-domain comparison and error. (a) Case IB-1; (b) case IB-2; (c) case IB-3; (d) frequency-domain error of test cases.

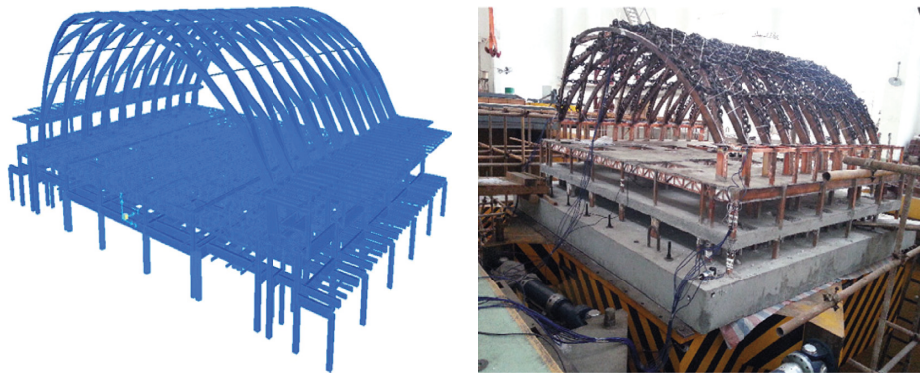

Figure 15: Shake table test with high-speed railway station specimen. (a) Numerical model; (b) test specimen.

3.6. Collision of Adjacent Multispan Bridges. A simplified test specimen of actual adjacent multispan bridges was established to study bridge collision under earthquake. The damping device for collision prevention is installed between two bridge girders. Two shake tables were used in the test to simulate adjacent two-span bridges' collision. Because of the importance of displacement in the collision test, the displacement instead of acceleration is adopted as the desired signal in the control of the shake table to reduce the displacement output error. Meanwhile, as there exist significant nonlinearities in the seismic collision and the nonlinear connection between pier and girder of the specimen, it is a challenge for shake tables to output the desired strong earthquake. However, the results of the test show a good performance of shake tables. The multispan bridge model is shown in Figure 22. The similarity ratio of this model is 1 : 6. The outputs of earthquake displacement and corresponding error of different earthquake test cases are

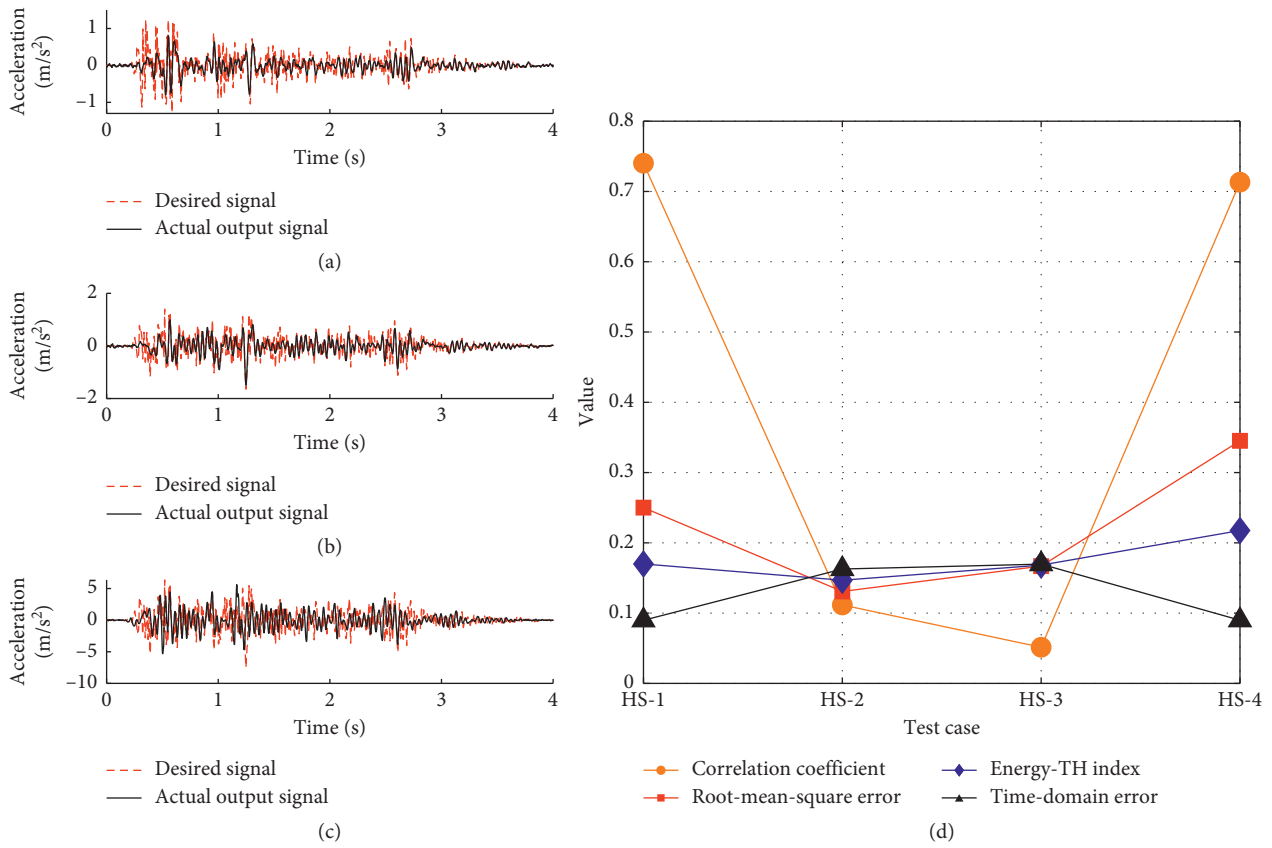

FIGURE 16: Shake table's output and corresponding error of different test cases with high-speed railway station. (a) Case HS-1; (b) case HS-3; (c) case HS-4; (d) output error of test cases.

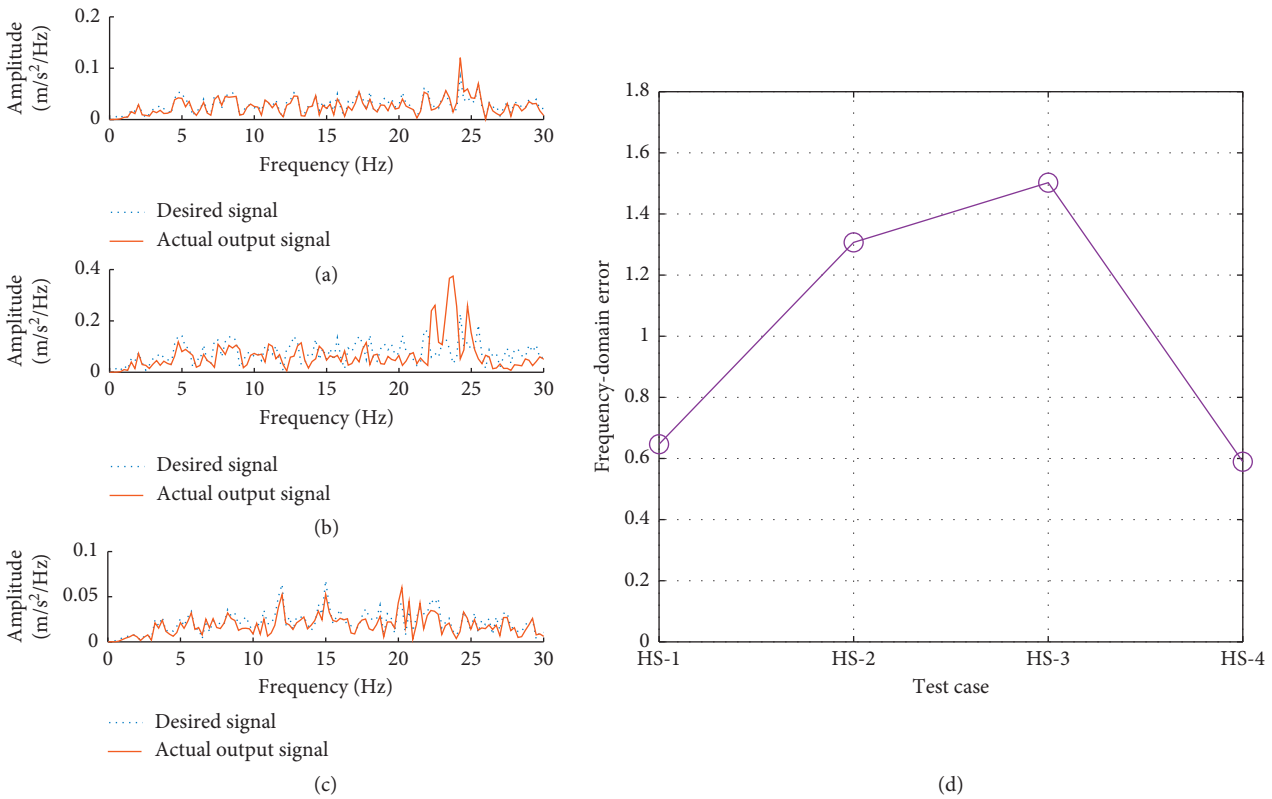

FIGURE 17: Desired signal and actual output signal frequency-domain comparison and error. (a) Case HS-1; (b) case HS-3; (c) case HS-4; (d) frequency-domain error of test cases.

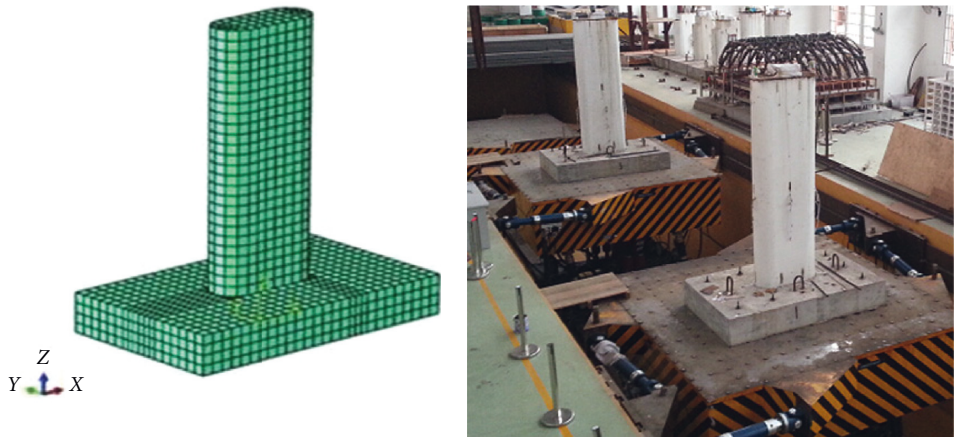

(a) (b)

Figure 18: Shake table test with high-speed railway bridge piers. (a) Numerical model; (b) test specimens.

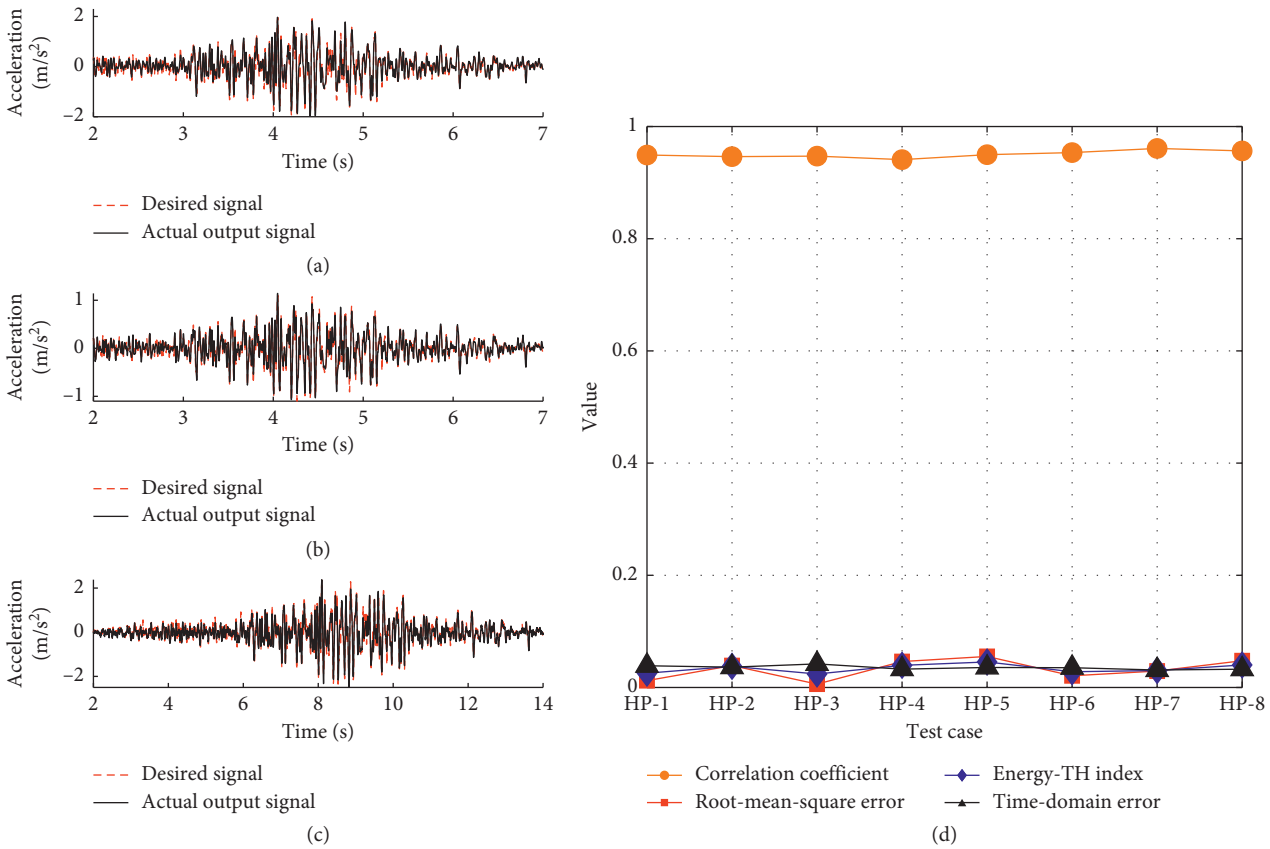

Figure 19: Shake table's output and corresponding error of different test cases with high-speed railway bridge piers. (a) Case HP-1; (b) case HP-3; (c) case HP-5; (d) output error of test cases.

shown in Figure 23. In these test cases, the maximum magnitude of displacement reaches 85 mm. The accuracy assessment adopts the reproduced displacement to calculate the error indices. The results show that the error of displacement output is approximately around 5%, and the shake table's output accuracy is good enough to complete the collision test. Correlation coefficients of seven cases are all close to 1, indicating that the similarity between desired and output signals is very high; the RMS error, the time-domain error, and the energy-TH index of seven cases are very close to 0, which means the difference between desired and output signals is very small. The RMS error and the energy-TH index of CB-3 are slightly higher than those of other cases. Hence, the error of signal reproduction has a slight influence on the structural response caused by the unexpected cumulative energy damage of the specimen. The energy of the

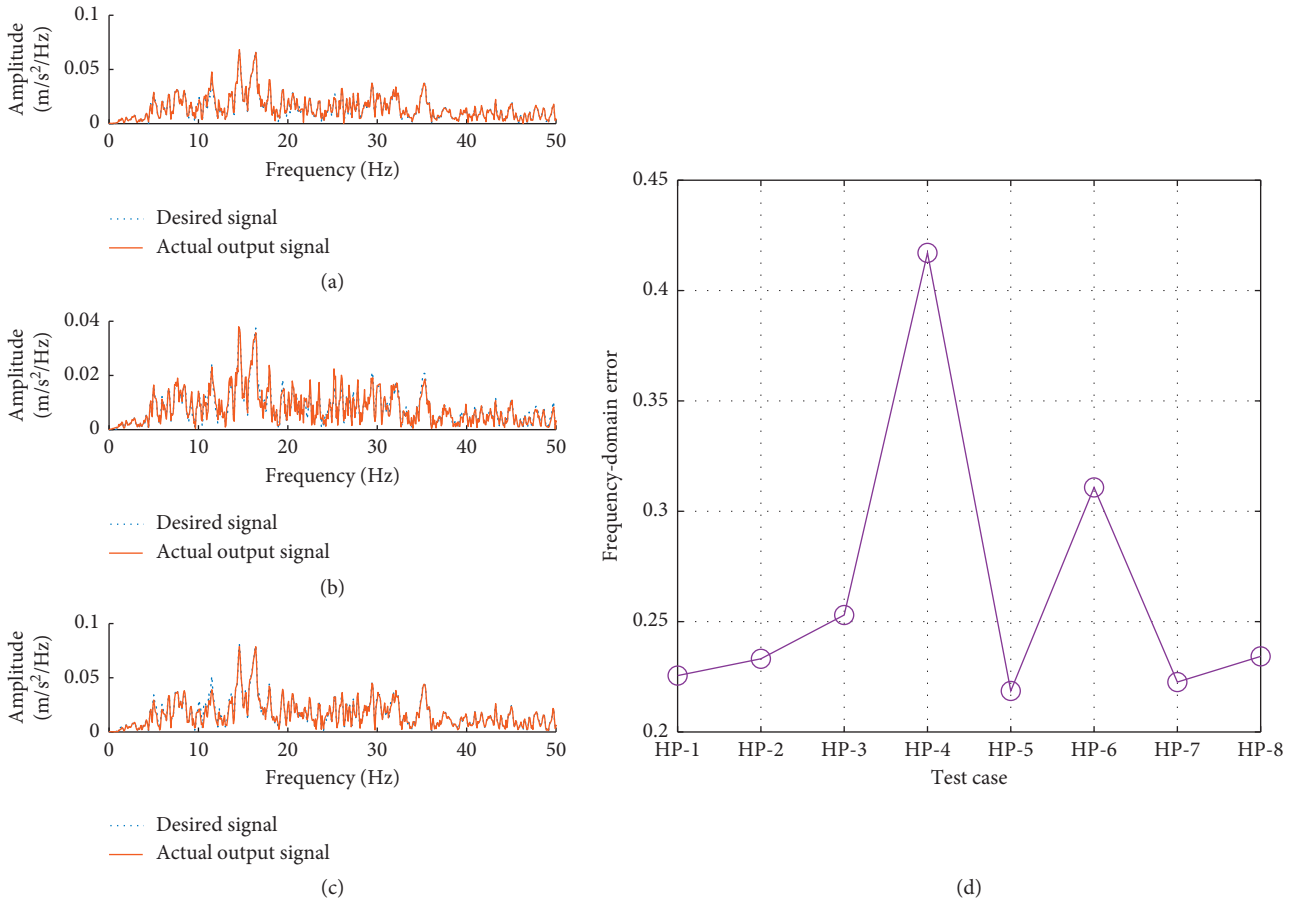

FIGURE 20: Desired signal and actual output signal frequency-domain comparison and error. (a) Case HP-1; (b) case HP-3; (c) case HP-5; (d) frequency-domain error of test cases.

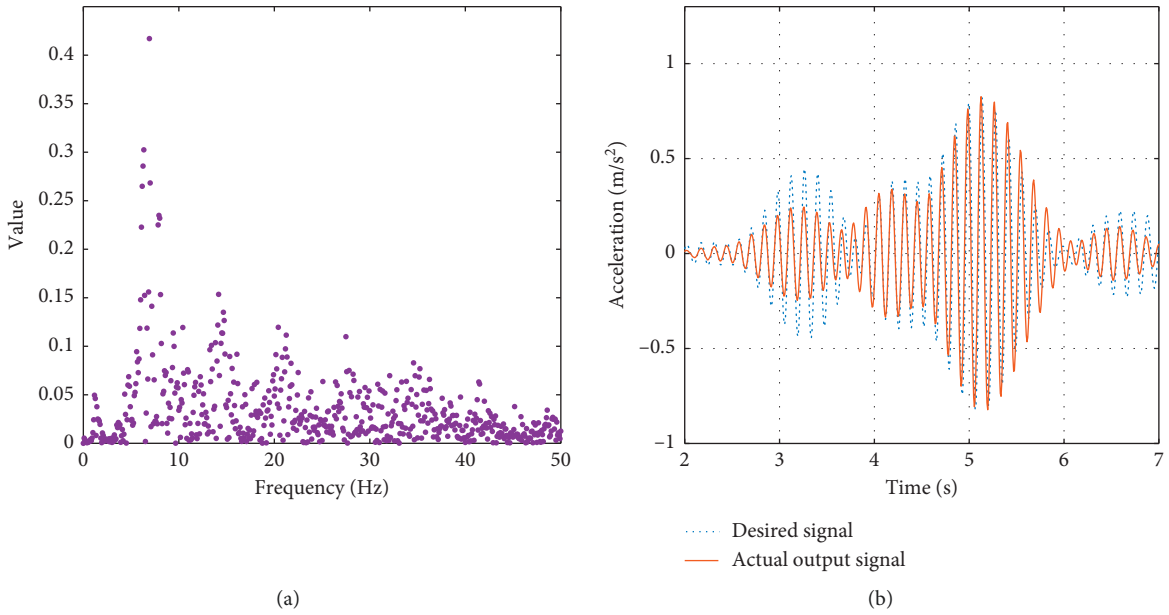

FIGURE 21: (a) Relative frequency error and (b) filtered time-history comparison of the desired signal and actual output signal of HP-4.

Figure 22: Shake table test with adjacent multispan bridges.

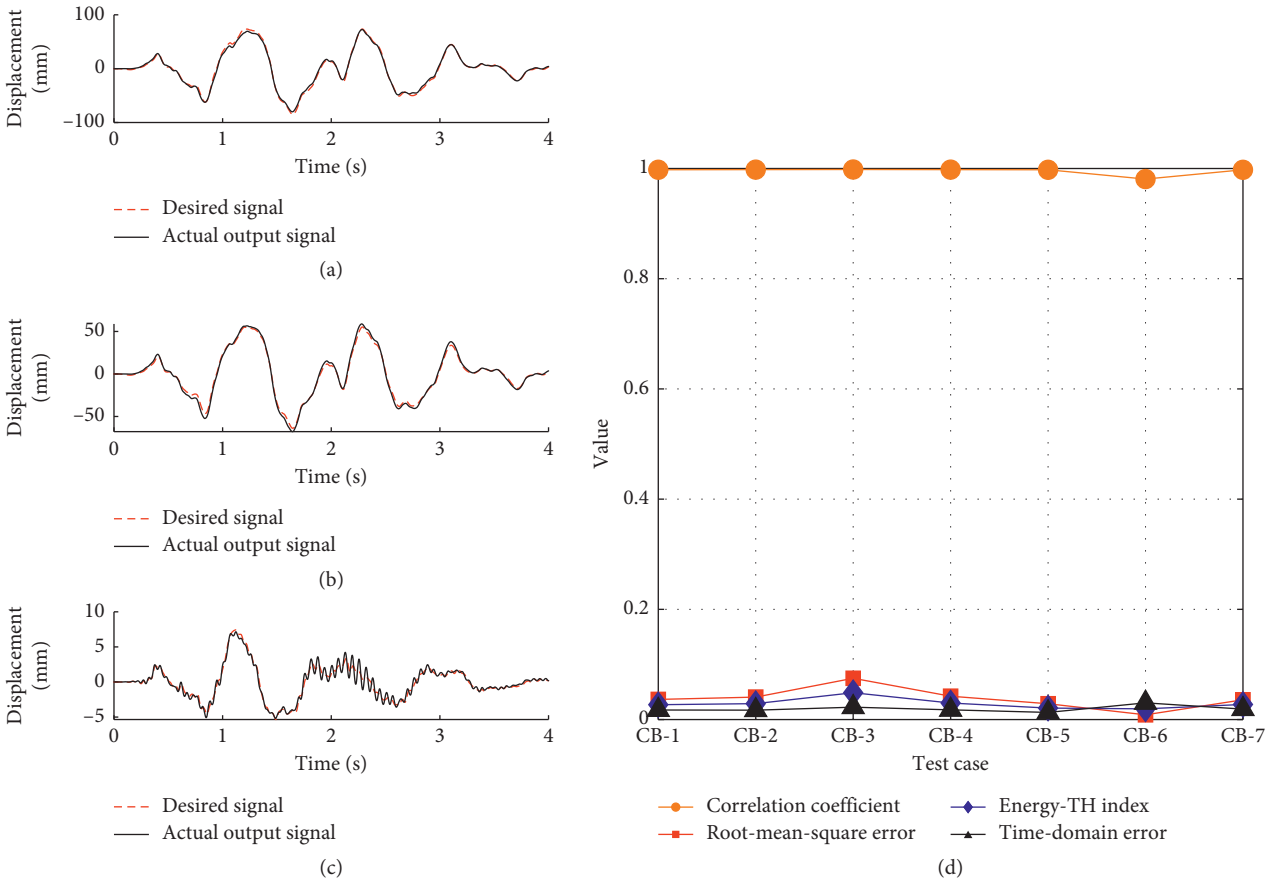

Figure 23: Shake table's output and corresponding error of different test cases with collision of adjacent multispan bridges. (a) Case CB-1; (b) case CB-3; (c) case CB-5; (d) output error of test cases.

desired signal is a little different from that of the output signal. Results show that the reproducing accuracy of the desired signals is good, and there is no significant difference among four indices.

Figure 24 gives the frequency-domain reproduction results of three test cases and the maximum frequency-domain error of all the test cases. CB-6 has the largest error in frequency domain, while the RMS error and the energy-TH index are the smallest. The maximum frequency-domain error of case CB-3 is also relatively high as for the RMS error and the energy-TH index. For the correlation coefficient, the error of CB-6 is larger than that of other test cases, which is like the trend of error in the frequency domain.

4. Structural Response Error Analysis

The main purpose of seismic signal reproduction on the shake table is to apply seismic excitation to the specimen and

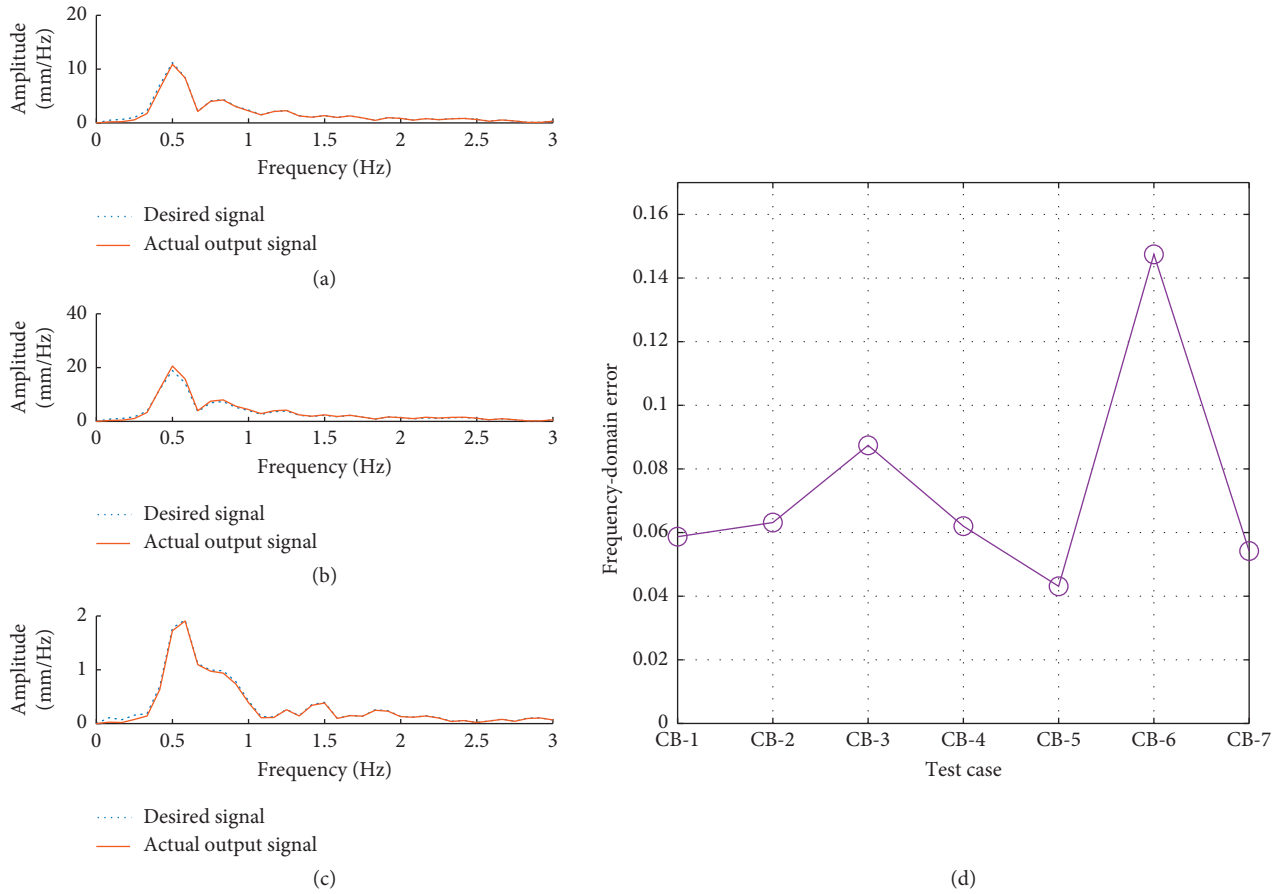

Figure 24: Desired signal and actual output signal frequency-domain comparison and error. (a) Case CB-1; (b) case CB-3; (c) case CB-5; (d) frequency-domain error of test cases.

then analyze the structural characteristics by studying the dynamic response of the specimen. The proposed index should be able to evaluate the seismic output accuracy on the aspect of the specimen. If the trend of the index is consistent with that of the structural response error, it shows that the index can reflect the influence of reproduction errors on the structural response. The shake table output accuracy of test HS is lower than other tests; hence, the difference between four indices should be more obvious. In order to fully evaluate the seismic reproduction accuracy of the shake table, the prototype finite element model corresponding to the HS was established to analyze the differences of structural dynamic responses excited by the desired signal and actual output signal.

The high-speed railway passenger station is a typical "building-bridge combination" frame structure, as shown in Figure 25, which is mainly composed of the rail layer, elevated layer, elevated interlayer, and roof.

To fully analyze the effects of energy-TH index from the aspect of maximum amplitude and energy, the nonlinear finite element model of HS is chosen. The elastic-plastic finite element model established on SAP 2000 is shown in Figure 15. Beams, columns, and large-span roof of this structure are simulated by using straight frame element. The nonlinear behavior of the specimen is expressed by plastic hinges. On both ends of elements of the roof, the fiber-coupled axial force and biaxial bending moment hinges (fiber P-M2-M3 hinge) are set.

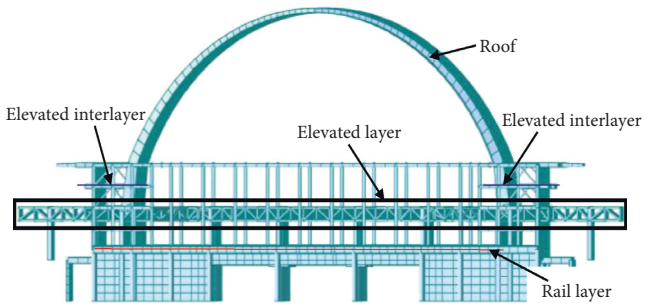

Figure 25: The high-speed railway passenger station.

The displacement response of the high-speed railway passenger station structure under ground motion is mainly concentrated at the top of the large-span roof, the middle of the elevated layer, the elevated interlayer, and the intersection of the elevated interlayer and large-span roof. The displacement response at the top of the large-span roof is the largest.

The desired signals and actual output signals in the HS test were selected as four sets of test cases. The excitation signals of the corresponding prototype structure are obtained by converting the four sets of signals according to the

similarity ratio. Then, four sets of excitation signals are applied to the finite element model to analyze the structural dynamic response. As shown in Figure 26, plastic hinges dissipate a part of energy conveyed from excited signals. The maximum displacement curves of the base shear force and the vertex corresponding to the excitation direction of the model are also obtained. The base shear is the shear force that the high-speed railway station structure bears. The top displacement refers to the displacement of the middle vertex of the roof of the high-speed railway station structure.

Considering the base shear of the HS under different ground motions and the vertex displacement at the vertex of the large-span roof, the structural response errors excited by desired signals and actual output signals are analyzed. The base shear and vertex displacement errors of the high-speed railway station prototype structure under four groups of excitation signals are calculated according to equation (4a), and the weighted sum of the errors of the two is taken into comprehensive consideration. The weight of both base shear and vertex displacement errors is 0.5, as shown in equation (4b), and the results are shown in Table 5:

$$\text{Error}_r = \frac{\max\left(r_d(t)\right) - \max\left(r_p(t)\right)}{\max\left(r_d(t)\right)}, \tag{4a}$$

$$\text{Error}_o = 0.5 * \text{Error}_{r,\text{dspl}} + 0.5 * \text{Error}_{r,\text{shear}}, \tag{4b}$$

where Error_r is the structural response error under the desired signal and actual output signal excitations, r_d is the structural dynamic response under the desired signal excitation, r_p is the structural response under actual output signal excitations, Error_o is the overall error of structural response including maximum vertex displacement error and base shear error, $\text{Error}_{r,\text{dspl}}$ calculated by using equation (4a) is the maximum vertex displacement (dspl) error under the desired signal and actual output signal excitations, and $\text{Error}_{r,\text{shear}}$ calculated by using equation (4a) is the base shear error under the desired signal and actual output signal excitations.

Table 6 gives the base shear error, vertex displacement response error, and energy-TH index of the prototype structure of high-speed railway station under four excitation signals. The structural response errors and four indices are compared according to the order of acceleration increase (Figure 27). As can be seen from Figure 27, the trend of energy-TH index is most consistent with the overall error of structural dynamic response, while the trend of time-domain error and correlation coefficient is contrary to the overall error trend of structural response. The energy-TH index is nearest to the error of structural response. Therefore, as an evaluation index of seismic reproduction accuracy of the shake table, the energy-TH index is better than correlation coefficient, time-domain error index, and RMS error.

5. Influence Analysis of Seismic Signal Parameters by b

Based on the proposed energy-TH index, the influence of seismic signal amplitude and frequency domain on shake table signal reproduction is studied. According to the selected test cases, the acceleration excitation and displacement excitation are analyzed, respectively.

For the case of seismic loading with acceleration, it can be seen from Figure 28 that the energy-TH index is distributed between 0 and 0.2 when the PGA is less than 3 m/s^2, while the energy-TH index is concentrated below 0.11 when the PGA is greater than 10 m/s^2. The energy-TH index decreases as the peak value of seismic acceleration increases. However, for the same test, there is no uniform linear relationship between energy-TH index and the PGA of the seismic signal. According to Figure 28 and Table 7, when the main frequency range of the seismic signal is 0.1~30 Hz, the energy-TH index falls in 0.14~0.22. When the main frequency range of the seismic signal is 0.1–50 Hz, the energy-TH index falls in 0.024~0.15, which is less than 0.1~30 Hz. When the main frequency range of the seismic signal is concentrated in 0.1~100 Hz (test LS), the energy-TH index is mainly distributed between 0.02 and 0.11. It is covered by the error range of test cases concentrated in 0.1–50 Hz, but the maximum error is smaller. Therefore, when acceleration is used as the excitation signal, the error scope tends to reduce with the increase of the peak value of earthquake and the frequency range of seismic signal coverage. The reproduction of signal, whose PGA less than 0.2g, may be affected by the mechanical and signal noise of the shake table equipment. The effect can be amplified by feedback control, which makes it possible that the precision of small amplitude signal reproduction is low. The energy-TH index of each test is relatively centralized relatively, which may be affected by different conditions of equipment and test experience of the experimenters and the inability of convergence to tolerance in ICS.

According to energy-TH index shown in Figure 29, for the case of seismic loading with displacement (test CB), the error increases with the increase of peak displacement. In these test cases, the main frequency range of the seismic displacement signal is concentrated at 0.1~3 Hz. The data are not enough to summarize the law between the accuracy of seismic displacement signal reproduction and the frequency range of seismic displacement signal.

6. Establishment of Double Parameter Performance Table

6.1. Comparison of Four Accuracy Assessment Indices. This paper analyzed several shake table tests of different structural types with four accuracy assessment indices, by which the performance of the shake table can be evaluated. The results show that energy-TH indices of most tests are controlled within 20%. The shake table using the ICS has good accuracy of strong earthquake output. In order to describe the performance of the shake table more reasonably and comprehensively, the double parameter performance table (Table 8) is given based on the energy-TH index and the correlation coefficient. The above 32 test cases are adopted to complete the table. It is obviously indicated by the energy-TH index that most tests can realize the accurate output of strong earthquake by using the shake table with

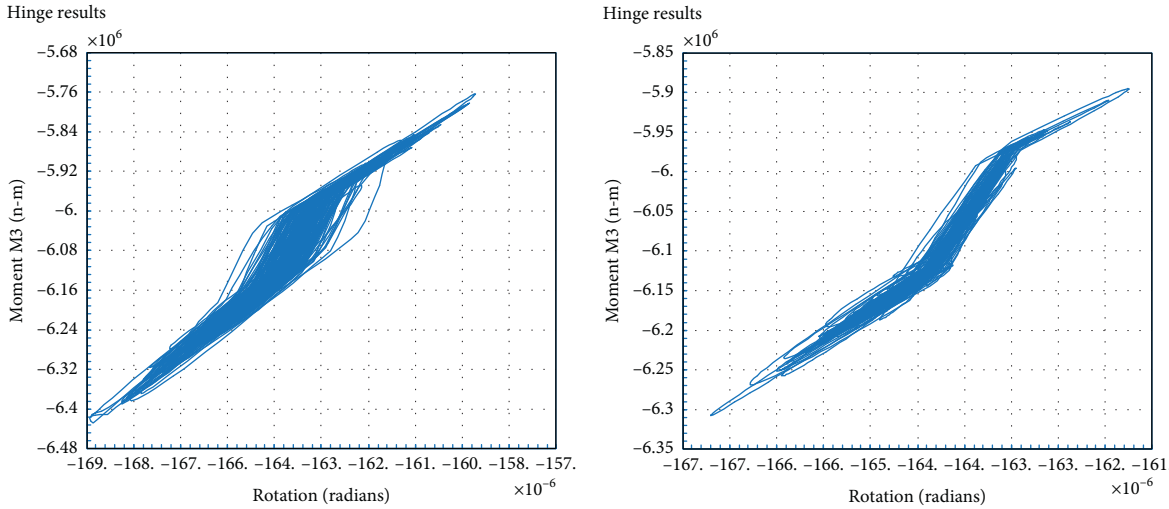

Figure 26: Moment rotation curves of a plastic hinge at the bottom of the roof. Case using (a) the desired signal as the excitation signal and (b) the actual output signal as the excitation signal.

Table 5: Structural response error of HS under the desired signal and actual output signal excitations.

Test case	Item	Desired signal	Actual output signal	$Error_r$	$Error_o$
HS-1	Maximum displacement (mm)	21	19	0.095	0.277
	Base shear (kN)	0.641*e*5	0.347*e*5	0.459	
HS-2	Maximum displacement (mm)	96	92	0.042	0.289
	Base shear (kN)	2.934*e*5	1.357*e*5	0.537	
HS-3	Maximum displacement (mm)	57	48	0.158	0.373
	Base shear (kN)	1.711*e*5	0.705*e*5	0.588	
HS-4	Maximum displacement (mm)	57	38	0.333	0.333
	Base shear (kN)	1.2954*e*5	0.864*e*5	0.333	

Table 6: Structural response error and other indices of HS.

Index	Error of structural response	Energy-TH index	Root-mean-square error	Time-domain error	Correlation coefficient
HS-1	0.277	0.16996	0.25011	0.08981	0.74016
HS-2	0.289	0.14680	0.13084	0.16276	0.11163
HS-3	0.373	0.168299	0.16690	0.16970	0.05142
HS-4	0.333	0.217543	0.34518	0.08990	0.71325

error less than 15%. Compared with the energy-TH index, the correlation coefficient is a stricter index. The error distribution diagrams based on the RMS error r and the time-domain error e are, respectively, shown in Figures 30 and 31. As mentioned in Section 2.3, the RMS error r represents the relative energy difference between the signals, and the time-domain error e represents the difference of signals over time. In Figure 20, it accounts for 56% of total tests when the RMS error is between 0 and 0.05. In Figure 31, it accounts for 69% of total tests when the time-domain error of the test is between 0 and 0.05. Figure 32 is drawn according to the correlation coefficient c in Table 8. In Figure 32, the correlation coefficient c of most cases are bigger than 0.9 when the energy-TH index b are between 0 and 0.05. c of 50% of tests is greater than 0.9, while c of 6% of tests is between 0.7 and 0.9. According to this table, the output accuracy of the shake table is higher under most test cases. The shake table test focuses on the structural damage, and the energy-TH index is appropriate and preferred for the accuracy assessment of earthquake output of the shake table. Using the double parameter performance table and massive test data, a more applicable and systematical table can be established to assess the shake table device. It can provide references for the applicability of future tests and benefit performance comparison of different shake table devices.

6.2. Output Accuracy Analysis of Shake Table Device. In this section, the comparison of the above 4 indices is given. For test cases of HP and CB, it is shown that the error of the strong earthquake output of the shake table can be controlled within 5%, and the correlation coefficient is around 0.95. It means the shake table has high accuracy of output. Hence, these test

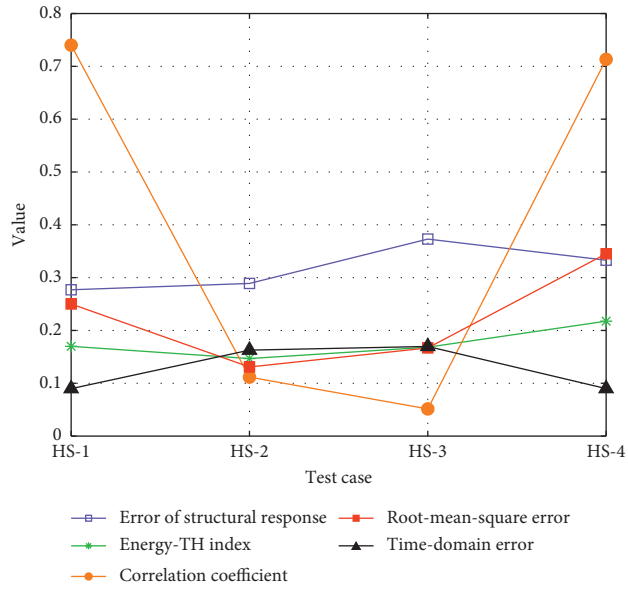

Figure 27: Comparison between structural response overall error and other indices of test HS.

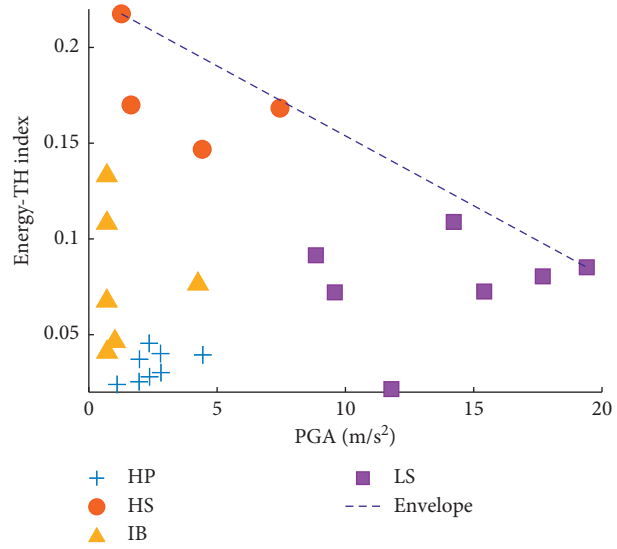

Figure 28: Energy-TH index of test cases under acceleration excitation.

Table 7: Energy-TH index of each case and frequency range of each test case.

Test	Signal type	Frequency range (Hz)	Energy-TH index of each case							
			Case 1	Case 2	Case 3	Case 4	Case 5	Case 6	Case 7	Case 8
HS	Acceleration	0.1–30	0.147	0.168	0.170	0.218	—	—	—	—
HP		0.1–50	0.024	0.025	0.028	0.030	0.037	0.039	0.040	0.045
IB		0.1–50	0.041	0.046	0.068	0.076	0.108	0.133	—	—
LS		0.1–100	0.021	0.072	0.073	0.080	0.085	0.091	0.109	—
CB	Displacement	0.1–5	0.019	0.021	0.027	0.027	0.029	0.030	0.049	—

cases of HP and CB would not be included in the comparison below. Six representative test cases are extracted from HS, LS, and IB. These cases are divided into two groups. The comparison of the 4 indices of the shake table is shown in Figure 33. The correlation coefficient is expressed by the correlation coefficient, which equals to $1 - c$.

Three test cases with smaller output errors are shown in Figure 33(a), in which the maximum RMS error is 0.25. The

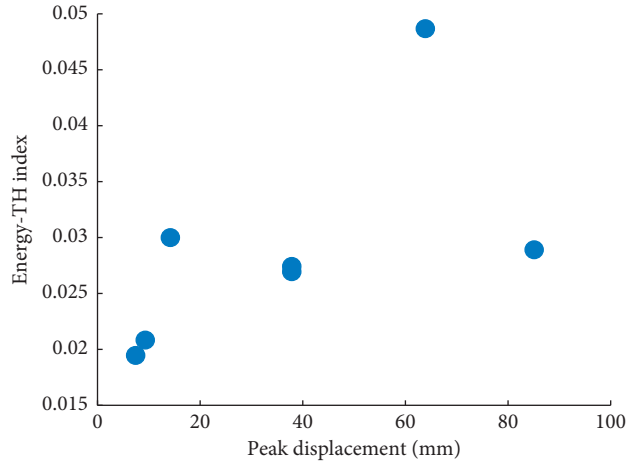

Figure 29: Energy-TH index of test cases under displacement excitation.

Table 8: Double parameter performance table for accuracy assessment of shake table devices.

Performance index 1		Correlation coefficient c				
Performance index 2		Level 1 ($0.95 < c \leq 1$)	Level 2 ($0.90 < c \leq 0.95$)	Level 3 ($0.85 < c \leq 0.90$)	Level 4 ($0.7 < c \leq 0.85$)	Level 5 ($c \leq 0.7$)
Energy-TH index b	Level 1 ($0 < b \leq 0.05$)	HP-6, HP-7, HP-8, CB-1, CB-2, CB-3, CB-4, CB-5, CB-6, CB-7	LS-3, HP-1, HP-2, HP-3, HP-4, HP-5	IB-5	IB-4	
	Level 2 ($0.05 < b \leq 0.1$)		LS-2	LS-1, LS-4, LS-7	LS-5, IB-1	IB-6
	Level 3 ($0.1 < b \leq 0.15$)			LS-6		IB-2, IB-3, HS-2
	Level 4 ($0.15 < b \leq 0.2$)				HS-1	HS-3
	Level 5 ($b > 0.2$)					HS-4

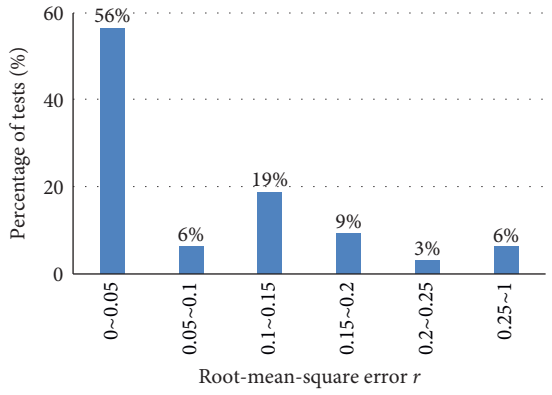

Figure 30: Root-mean-square error distribution diagram of different test cases.

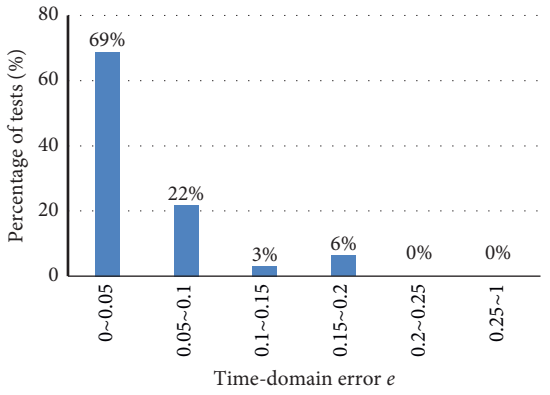

Figure 31: Time-domain error distribution diagram of different test cases.

other three cases shown in Figure 33(b) have larger errors. The maximum RMS error in Figure 33(b) is 0.35, which indicates that there may be test failure and accidental structural damage. The energy and the amplitude of desired signals are comprehensively considered by energy-TH index b, which is a reasonable index from the point of view of structural seismic damage. In Figure 33, the correlation coefficient $1-c$ is greater than the energy-TH index b in three test cases. If $1-c$ is adopted, the results of shake table test evaluation may be misjudged even though the response of the specimen is consistent with the expectation.

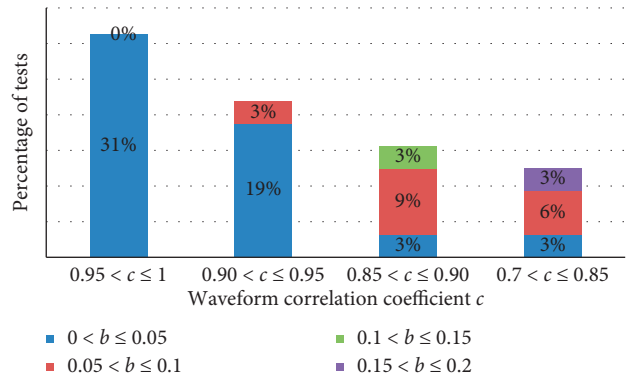

Figure 32: Accuracy distribution diagram based on correlation coefficient.

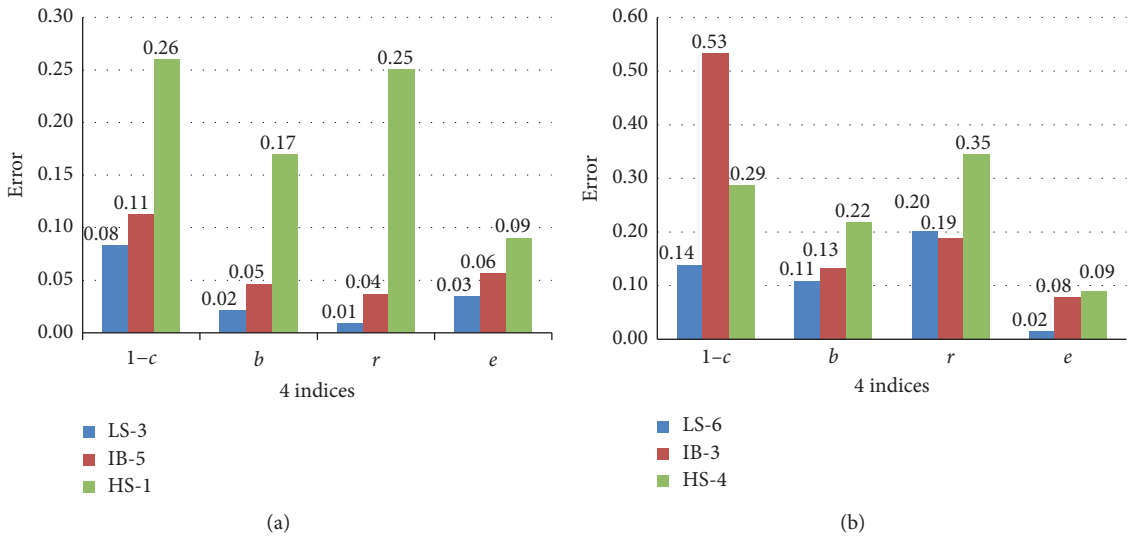

Figure 33: Comparison of shake table output error indices of several test cases. Test cases with (a) relatively small output error and (b) relatively big output error.

7. Conclusions

Based on the shake table tests of several typical civil engineering structures, this paper systematically evaluates the strong earthquake output accuracy of the shake table, puts forward the energy-TH index, and establishes the performance table of double index parameters. The following conclusions are given: (1) The nonlinearity of the shake table and specimens has influence on the large earthquake output. The accuracy of the strong earthquake output is generally related to the shake table performance, weight and stiffness of specimens, shake table-specimen interaction, and earthquake outputs. (2) The transfer function obtained under small excitation input and the drive signal obtained by ICS are feasible for strong earthquake output. Mostly the energy-TH index can be controlled within 20%. (3) The finite element model of HS is established to analyze the structural response of the desired signal and output signal of the shake table. Compared with other indices, the proposed energy-TH index is closer to the structural response error. The energy-TH index is more reasonable than other indices. (4) The influence of PGA and frequency range of the seismic signal on output accuracy of the shaking table is evaluated based on the energy-TH index. It is found that, for the case of acceleration as the excitation signal, the larger the PGA is, the smaller the overall error is, and the frequency range has no obvious influence on the shake table output accuracy.

Data Availability

The numeric data used to support the findings of this study may be released upon application to the author, who can be contacted at guowei@csu.edu.cn.

Conflicts of Interest

The authors declare that they have no conflicts of interest.

Acknowledgments

This work was supported by the National Natural Science Foundation of China (grant no. 51108466), Development Program for Changjiang Scholars and Innovative Team (grant no. IRT1296), and Project of Innovation-Driven Plan

in Central South University. These supports are gratefully acknowledged.

References

[1] W. Guo, Y. Hu, Y. Li, Z. Zhai, and P. Shao, "Seismic performance evaluation of typical dampers designed by Chinese code subjected to the main shock-aftershocks," *Soil Dynamics and Earthquake Engineering*, vol. 126, Article ID 105829, 2019.

[2] W. Guo, Z. Zhai, Y. Cui, Z. Yu, and X. Wu, "Seismic performance assessment of low-rise precast wall panel structure with bolt connections," *Engineering Structures*, vol. 181, pp. 562–578, 2019.

[3] W. Guo, C. Zeng, H. Gou, Y. Hu, H. Xu, and L. Guo, "Rotational friction damper's performance for controlling seismic response of high speed railway bridge-track system," *Computer Modeling in Engineering & Sciences*, vol. 120, no. 3, pp. 491–515, 2019.

[4] E. Sloane and C. Heizman, "System for digitally controlling a vibration testing environment or apparatus," U.S. Patent No. 3,710,082. U.S. Patent and Trademark Office, Washington, DC, USA, 1973.

[5] M. Blondet and C. Esparza, "Analysis of shaking table-structure interaction effects during seismic simulation tests," *Earthquake Engineering & Structural Dynamics*, vol. 16, no. 4, pp. 473–490, 1988.

[6] D. P. Newell, H. L. Dai, M. K. Sain, P. Quast, and B. F. Spencer, "Nonlinear modeling and control of a hydraulic seismic simulator," in *Proceedings of the 1995 American Control Conference*, vol. 1, pp. 801–805, Seattle, WA, USA, June 1995.

[7] J. P. Conte and T. L. Trombetti, "Linear dynamic modeling of a uniaxial servo-hydraulic shaking table system," *Earthquake Engineering & Structural Dynamics*, vol. 29, no. 9, pp. 1375–1404, 2000.

[8] N. Ogawa, K. Ohtani, I. Nakamura, E. Sato, and T. Nagasaki, "Development of core technology for 3-d 1200 tonne large shaking table," in *Proceedings of 12th World Conference on Earthquake Engineering*, Auckland, New Zealand, 2000.

[9] T. L. Trombetti and J. P. Conte, "Shaking table dynamics: results from a test-analysis comparison study," *Journal of Earthquake Engineering*, vol. 6, no. 4, pp. 513–551, 2002.

[10] J. G. Chase, N. H. Hudson, J. Lin, R. Elliot, and A. Sim, "Nonlinear shake table identification and control for near-field earthquake testing," *Journal of Earthquake Engineering*, vol. 9, no. 4, pp. 461–482, 2005.

[11] Y. Tagawa and K. Kajiwara, "Controller development for the E-defense shaking table," *Proceedings of the Institution of Mechanical Engineers, Part I: Journal of Systems and Control Engineering*, vol. 221, no. 2, pp. 171–181, 2007.

[12] A. R. Plummer, "A detailed dynamic model of a six-axis shaking table," *Journal of Earthquake Engineering*, vol. 12, no. 4, pp. 631–662, 2008.

[13] A. R. Plummer, "Control techniques for structural testing: a review," *Proceedings of the Institution of Mechanical Engineers Part I-Journal of Systems and Control Engineering*, vol. 221, no. I2, pp. 139–169, 2007.

[14] H. Zhou, S. Xiaoyun, T. Yingpeng et al., "Reproducing response spectra in shaking table tests of nonstructural components," *Soil Dynamics and Earthquake Engineering*, vol. 127, Article ID 105835, 2019.

[15] F. De Coninck, W. Desmet, and P. Sas, "Increasing the accuracy of MDOF road reproduction experiments: calibration, tuning and a modified TWR approach," in *Proceedings of the ISMA 2004*, pp. 709–722, Leuven, Belgium, 2004.

[16] M. A. Underwood, *Jaguar Systems On-Line Operating Manuals: MIMO Waveform Replication*, Spectral Dynamics Inc., San Jose, CA, USA, 2003.

[17] G. Guan, W. Xiong, H. Wang, and H. Junwei, "6 degree0f-freedom long-term waveform replication control," in *Proceedings of the International Conference on Information Engineering & Computer Science*, IEEE, Wuhan, China, December 2009.

[18] J. Y. Zhang, R. Gao, J. Hu et al., "Application comparison of grey correlation degree and Pearson correlation coefficient," *Journal of Chifeng University*, vol. 30, no. 11, 2014, in Chinese.

[19] Y.-J. Park and A. H. S. Ang, "Mechanistic seismic damage model for reinforced concrete," *Journal of Structural Engineering*, vol. 111, no. 4, pp. 722–739, 1985.

[20] W. Guo, Y. Hu, H. Liu, and B. Dan, "Seismic performance evaluation of typical piers of China's high-speed railway bridge line using pushover analysis," *Mathematical Problems in Engineering*, vol. 2019, Article ID 9514769, 17 pages, 2019.